NRL Report 6541

# Calculations Useful in the Determination of Electron Temperature from X-Ray Continuum Radiation Emitted from High Temperature Plasmas

R. C. Elton and A. D. Anderson

*Plasma Physics Branch*
*Plasma Physics Division*

March 31, 1967

APPROVED FOR PUBLIC RELEASE - DISTRIBUTION UNLIMITED

**NAVAL RESEARCH LABORATORY**
**Washington, D.C.**

DISTRIBUTION OF THIS DOCUMENT IS UNLIMITED

CONTENTS


| | |
|---|---|
| Abstract | ii |
| Problem Status | ii |
| Authorization | ii |
| INTRODUCTION | 1 |
| DESCRIPTION OF CALCULATIONS | 2 |
| DISCUSSION | 2 |
| REFERENCES | 4 |

## ABSTRACT

The results of calculations of the total integrated bremsstrahlung radiation passing through absorbing foils of beryllium, aluminum, and nickel [as well as aluminum and nickel in combination with carbon (polyethylene)] are presented for various temperatures and a range of useful thicknesses. Such information is necessary in obtaining values for the electron temperature in a plasma from measurements of the soft x-ray continuum emission. The spectral distribution of the transmitted radiation is also presented for use in determining the spectral region observed, thereby avoiding regions of undesirable radiation. An indication of an observable flux level in a typical experiment is given, along with equations suitable for scaling to other plasma conditions, as a further aid in selecting foils for a particular application.

## PROBLEM STATUS

This is a final report on one phase of the problem of electron temperature determination in a plasma.

## AUTHORIZATION

NRL Problem H02-24
Project RR 002-10-45-5054

Manuscript submitted January 18, 1967.

# CALCULATIONS USEFUL IN THE DETERMINATION OF ELECTRON TEMPERATURE FROM X-RAY CONTINUUM RADIATION EMITTED FROM HIGH TEMPERATURE PLASMAS

## INTRODUCTION

Plasmas at temperatures greater than $kT = 100$ eV ($T = 1.2 \times 10^6$ °$K$) are characterized by a strong x-ray continuum spectrum (as well as characteristic line radiation from optical transitions in impurity ions). The bremsstrahlung continuum intensity per wavelength interval is given by (1,2)

$$I_\lambda = C \frac{n_i n_e Z^2 c \ell}{\lambda^2 \sqrt{kT}} \overline{g_{ff}} \exp(-E/kT), \tag{1}$$

where $E$ represents the x-ray photon energy, $\lambda$ is the corresponding wavelength, $T$ is the electron temperature, $n_i$ and $n_e$ are the ion and electron densities respectively, $\ell$ is the effective plasma length, $Z$ is the nuclear charge (1 for hydrogen and deuterium), $\overline{g_{ff}}$ is the mean Gaunt factor for free-free transitions, and $C$ is a constant given by

$$C = \frac{32 \pi^2 e^6}{3\sqrt{3}\, c^3 (2\pi m)^{3/2}} = 6.36 \times 10^{-47} \text{ [cgs units]}, \tag{2}$$

where $c$ is the velocity of light and $k$ is the Boltzmann constant.

Thus, the high-energy cutoff for x-radiation in the 1 keV range at temperatures above that given by $kT = 100$ eV is quite sharp as indicated by the exponential and is strongly dependent upon temperature. This dependence of the high-energy cutoff on temperature has been used as the basis of a technique for temperature measurement; i.e., a determination of the high-energy continuum wavelength distribution affords a rather sensitive measurement of the plasma electron temperature (2-6).

Since x-ray spectrometers are generally of very low efficiency, measurements of the continuum radiation are often obtained with broadband filters constructed from thin metallic foils. Thus, a comparison of the intensities transmitted through foils of various materials and various thicknesses is often satisfactory for determining the wavelength distribution of the continuum intensity and, thereby, the electron temperature.

This report presents results of the calculations of the wavelength distribution of the specific bremsstrahlung continuum radiation per unit wavelength interval in the soft x-ray spectral region transmitted through various metallic filters, as well as calculations of the ratio of the integrated intensity through the foils to the total (integrated) incident continuum radiation. Results are presented for foils of beryllium, aluminum, and nickel, as well as combinations of carbon (polyethylene) with both nickel and aluminum. Some typical ratios (useful in obtaining temperature values) of the integrated transmitted intensities for various foil thicknesses as a function of temperature are presented and discussed. Data on the x-ray flux emitted from the NRL 2-MJ theta-pinch device is also presented. This can be scaled to other plasma conditions as a guide in selecting appropriate foils.

## DESCRIPTION OF CALCULATIONS

The specific intensity ($I'_\lambda$) at any particular wavelength, transmitted through absorbing foils of thickness $D_j$ with an absorption coefficient $K_j$, is given by the product of Eq. (1) and the total foil transmission, $\exp[-K_j(E)D_j]$; or,

$$I'_\lambda = C\frac{n_i n_e Z^2 c\ell}{\lambda^2\sqrt{kT}}\overline{g_{ff}}\exp\left[-E/kT - \sum_j K_j(E)D_j\right], \tag{3}$$

where the subscript $j$ refers to the various foil materials. The high-energy (low-wavelength) cutoff is still given by the exponential energy function. However, the long-wavelength cutoff is now determined by the characteristics of the absorbing foil.

Values of Eq. (3) have been calculated, using the NRL NAREC computer, for a range of foil thicknesses, various foil materials, and several temperatures. (A graph for converting foil thickness expressed in mg/cm$^2$ into inches is given for convenience in Fig. 1, where the specific gravities were obtained from Ref. 8, and a value of unity was used for carbon.)

These values were automatically plotted versus wavelength, and the results are given in Figs. 2 through 21. Such graphs are most useful in determining the wavelength region observed, thereby assuring the avoidance of regions of characteristic line radiation. For example, resonance radiation from OVII and OVIII (16 to 22 Å) can seriously compete in intensity with the underlying and nearby continuum intensity, even in systems where oxygen exists in minute amounts. This contribution from line radiation can be made negligible by using thick foils (where the x-ray flux is sufficient) or by combining, for example, aluminum or nickel with carbon in the convenient form of polyethylene ($CH_2$) as shown in Figs. 10 through 13 and 18 through 21.

Absorption coefficients for aluminum, beryllium, and carbon, used in the numerical calculations, were taken from a compilation due to Gilmore (7). Nickel absorption coefficients were obtained from Allen (8) for wavelengths shorter than the L edge at 12.3 Å. For longer wavelengths, values were obtained from those measured for copper (9) by multiplying by 0.91,* a procedure expected to be accurate to 5%.

A numerical integration of Eq. (3) over a photon energy ($E = hc/\lambda$) range of 0.1 keV to 10 keV, with a mesh equivalent to an energy interval of 50 eV near absorption edges, was carried out initially on the NRL NAREC computer and, more recently, on the NRL-CDC-3870 computer. The normalized total transmission, given by the integral of Eq. (3) divided by the integral of the incident pure bremsstrahlung radiation ($D_j = 0$), is plotted versus foil thickness for various temperatures in Figs. 22 through 27 for the same foil materials described in the previous figures. From these graphs, plots of the integrated foil transmission versus temperature may be obtained for any desired foil thickness. More important, ratios of transmission for two different foils may be obtained such as are shown typically in Figs. 28 and 29. A study of these latter figures is useful for determining the temperature range of greatest sensitivity in selecting a particular foil combination, as discussed below.

## DISCUSSION

The results of the calculations just described, which are presented in the following graphs, are useful in the initial conception and design of an experiment to measure the electron temperature in a plasma and are useful in the final analysis of the relative x-ray continuum intensities measured through thin metallic absorbing foils. Typically, materials

*The authors are grateful to N. J. Peacock of Culham Laboratory for suggesting this approach.

are first selected and thicknesses tentatively assigned consistent with a suspected contribution from line radiation both in the x-ray region of interest as well as in other spectral regions in which the foils may have significant transmission. For example, several types of foil considered here such as aluminum, beryllium, and carbon have a transmission window in the region of 150 to 170 Å. The presence of oxygen impurity ions in the plasma will often produce copious amounts of OV and OVI radiation in this spectral region, perhaps from cooler layers in the field of view, which will also pass through the filters to some degree.

Comparison of signals with those obtained through foils such as nickel which is opaque in the 150 Å region will often indicate any difficulties due to these effects (6). The possibility of penetration of charged particles through the foils makes additionally desirable the use of as great a foil thickness as possible for the available x-ray flux.

The proper choice of foil thickness therefore depends on the available radiation flux from the source and the available detector sensitivity, factors which ultimately place an upper limit on the useful foil thickness. Indicated in Figs. 22 through 27 by arrows (as well as in Figs. 28 and 29 by the dashed portions of the curves) is a somewhat arbitrary lower level of sensitivity of $4 \times 10^{-4}$ as determined from a particular experiment, i.e., for a four-channel detection system (6) used in conjunction with the NRL large Pharos theta-pinch device (10).

In this system, the x-rays were viewed through a combination of metallic foil, scintillator, mirror, and photomultiplier having a conical field of view describing a solid angle of 0.09 steradians and an aperture diameter at the foil of 1.6 mm. This system gave a lower limit to the useful total bremsstrahlung transmission of approximately $4 \times 10^{-4}$ with an EMI type 6255B photomultiplier operated at -1600 V and with an NE-102 plastic scintillator. This transmission limit depends upon plasma conditions which were as follows: $kT_e$ = 900 eV, $n_i = n_e = 10^{17}\,\mathrm{cm}^{-3}$, and $\ell$ = 100 cm. The nickel foil used in determining these limits was of thickness 6.8 mg/cm$^2$. From this information and Eq. (3), the minimum intensity may be scaled to other devices in order to obtain a rough estimate of the thickest foil likely to transmit measurable radiation for any particular experiment. (See discussion below concerning the Gaunt factors.)

Thus, having determined the most desirable material and maximum foil thickness usable, the information in Figs. 22 through 27 may be used to plot the ratio of integrated intensity transmitted for two different foils as a function of temperature; typical examples are shown in Figs. 28 and 29 for beryllium and aluminum. From curves such as these, the thicknesses used may be again adjusted to obtain maximum sensitivity of the temperature determination for the region of interest.

It should be pointed out that the transmission curves for specific intensity versus wavelength (Figs. 2 through 21) may be combined to yield the transmission through stacked foils, using the zero-thickness pure bremsstrahlung ($D_j = 0$) curves for normalization. However, the integrated intensity data shown in Figs. 22 through 27 is not so easily combined and generally must be computed for each specific combination. (See Ref. 2, chapter 13, for an analytical method of integration when absorption edges do not occur in the region of interest.)

Recombination continuum radiation into oxygen states of high ionization will naturally contribute to the continuum intensity below the relevant series limits. However, the exponential function given in Eqs. (1) and (3) will continue to hold for recombination radiation, as well as for free-free bremsstrahlung continuum radiation. The free-bound (as well as the free-free) Gaunt factors are not known for the oxygen ions. However, since the Gaunt factors always appear in ratios between foils for the temperature measurement, errors in the deduced temperature due to the noninclusion of a wavelength-dependent Gaunt factor

in the integration will be less than 10 percent, particularly if the radiation passbands are chosen close together and in regions of slowly varying Gaunt factors (2).

## REFERENCES


1. Elton, R.C., "Stark Profile Measurement of the Lyman-$\alpha$ and Lyman-$\beta$ Lines of Hydrogen," NRL Report 5967, July 1963. The factor $\exp(-h\nu/kT)$ was inadvertently omitted in going from Eq. (13) to Eq. (14) in this report.

2. Griem, H.R., "Plasma Spectroscopy," New York:McGraw-Hill, 1964

3. Jahoda, F.C., Little, E.M., Quinn, W.E., Sawyer, G.A., and Stratton, T.F., Phys. Rev. 119:843 (1960)

4. Griem, H.R., Kolb, A.C., Lupton, W.H., and Phillips, D.T., Nuclear Fusion Supplement, Part 2, p. 543, (1962)

5. Peacock, N.J., Culham Laboratory Report CLM-M-39, 1964

6. Elton, R.C., Hintz, E., and Swartz, M., "Proceedings Seventh International Conference on Phenomena in Ionized Gases," Vol. 3, Belgrade:Gradevinska Knjiga Publ. House, p. 190, 1966

7. Gilmore, F.R., "Graphs of X-Ray Absorption Coefficients for Fourteen Substances," Research Memorandum RM-2367-AEC, Apr. 1959

8. "Handbook of Chemistry and Physics," 45th edition 1964-1965, Cleveland:Chemical Rubber Co., 1964

9. Cooke, B.A., and Stewardson, E.A., Brit. J. Appl. Phys. 15:1315 (1964)

10. Kolb, A.C., Lupton, W. H., Elton, R.C., McLean, E.A., Swartz, M., Young, M.P., Griem, H.R., and Hintz, E., "Plasma Physics and Controlled Nuclear Fusion Research," Vol. 1, Vienna:International Atomic Energy Agency, p. 261, 1966

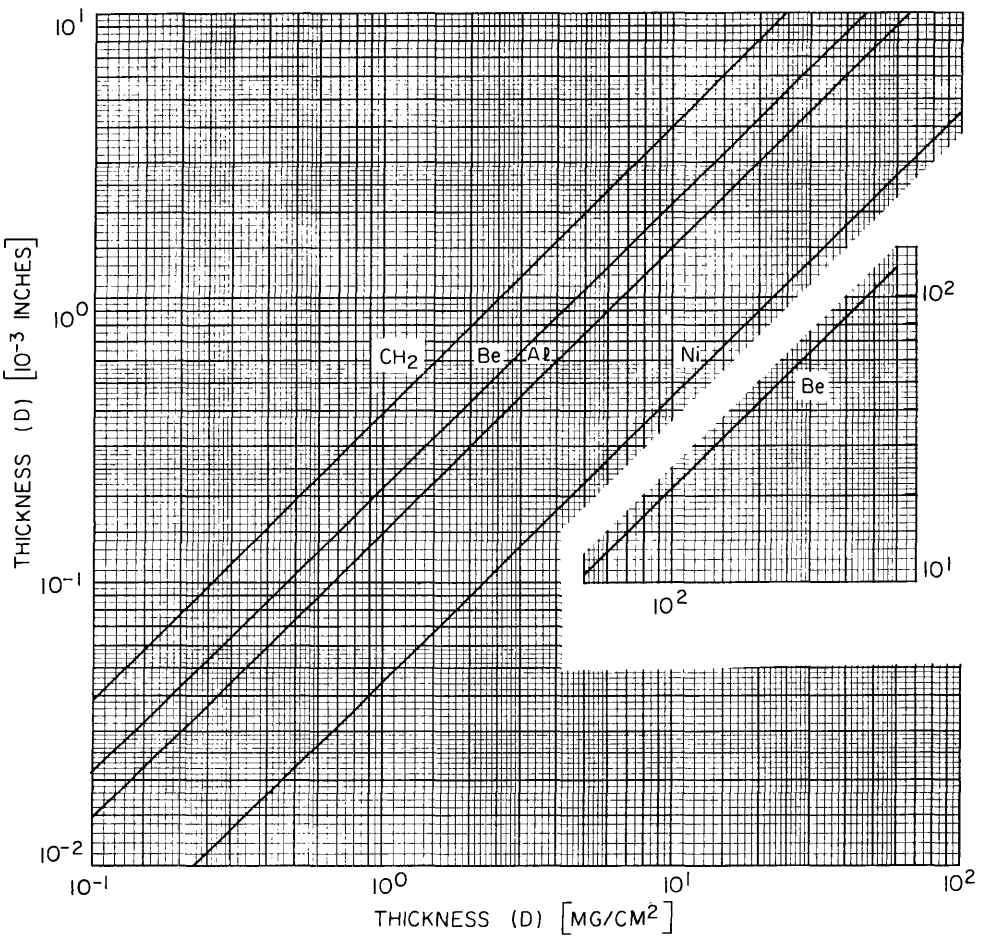


Fig. 1 - Graph for converting foil thicknesses expressed in mg/cm$^2$ into inches for various foil materials. For polyethylene ($CH_2$) a specific gravity of unity is assumed.

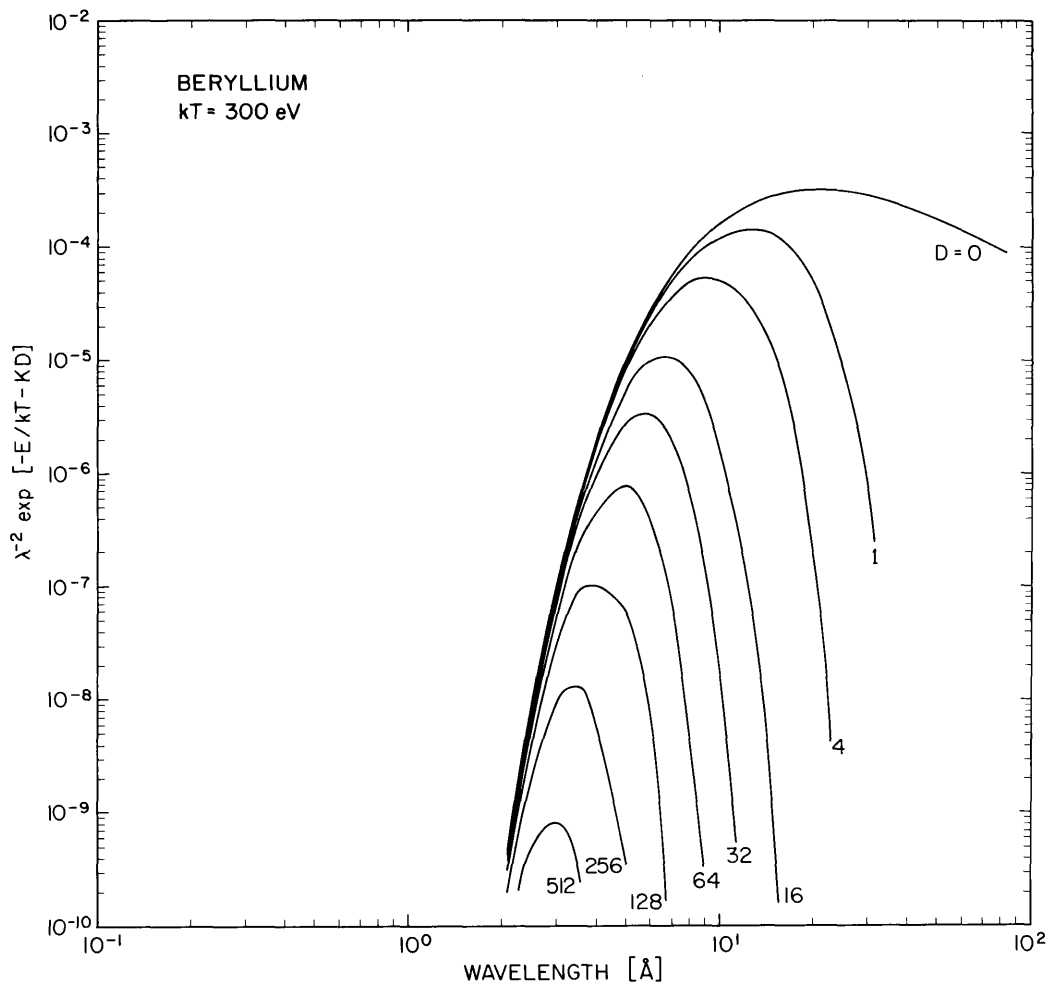


Fig. 2 - Relative bremsstrahlung emission at a temperature ($T$) transmitted through beryllium absorbing foils of thickness ($D$) versus wavelength

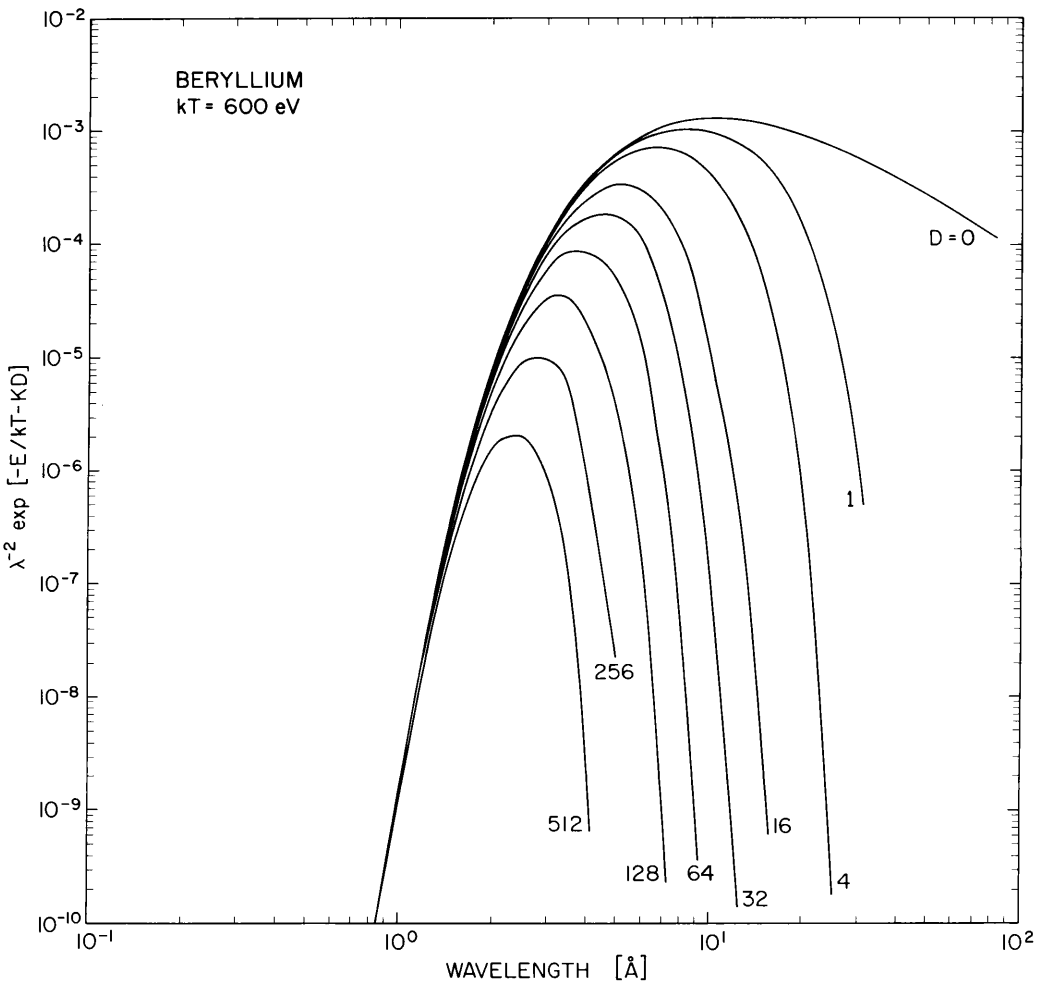


Fig. 3 - Relative bremsstrahlung emission at a temperature ($T$) transmitted through beryllium absorbing foils of thickness ($D$) versus wavelength

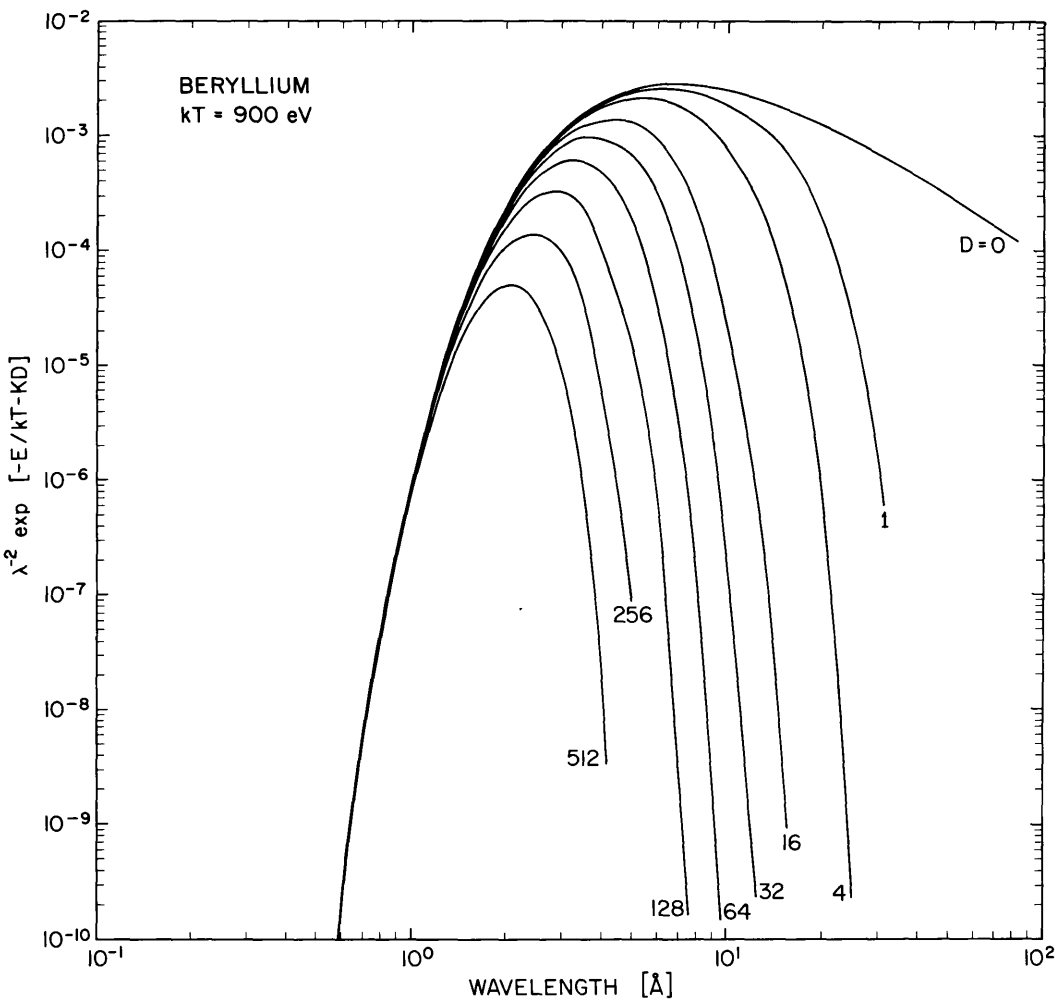


Fig. 4 - Relative bremsstrahlung emission at a temperature ($T$) transmitted through beryllium absorbing foils of thickness ($D$) versus wavelength

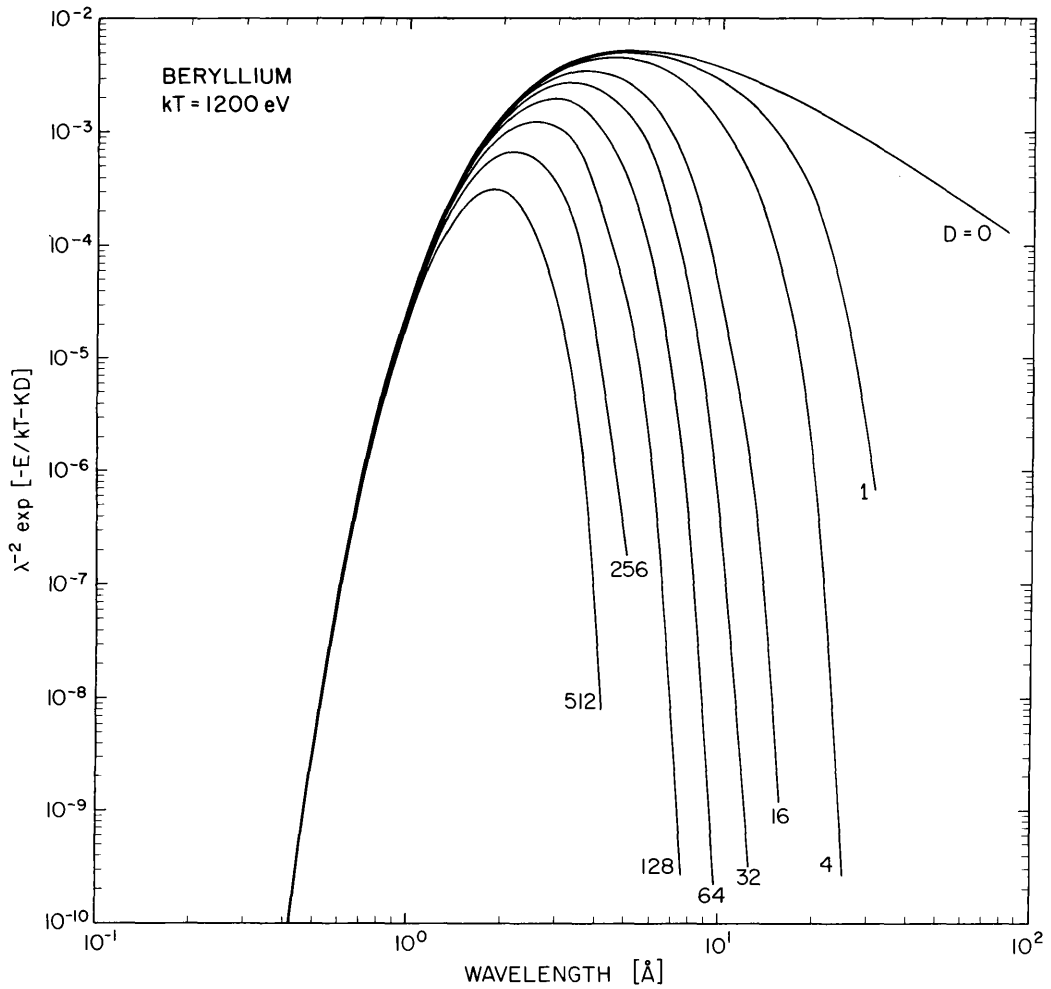


Fig. 5 - Relative bremsstrahlung emission at a temperature ($T$) transmitted through beryllium absorbing foils of thickness ($D$) versus wavelength

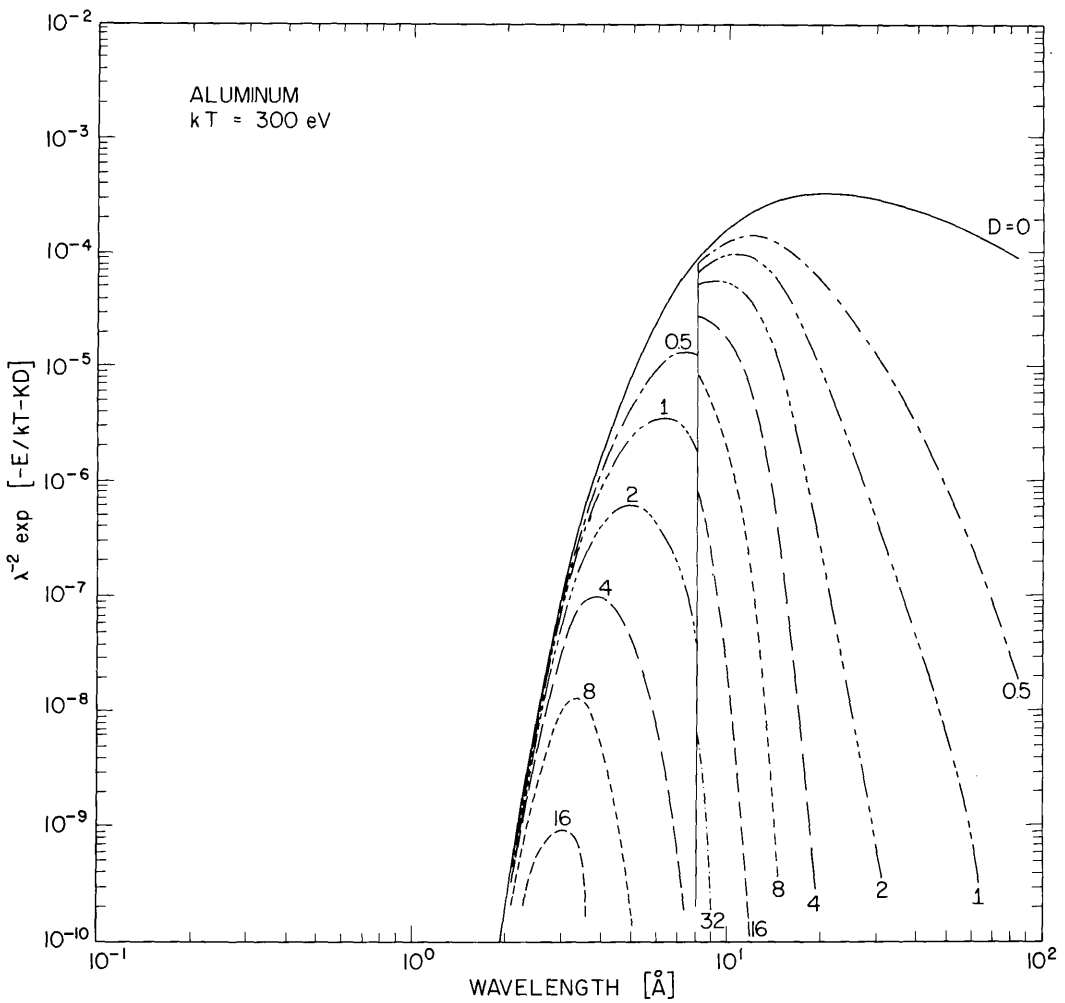


Fig. 6 - Relative bremsstrahlung emission at a temperature ($T$) transmitted through aluminum absorbing foils of thickness ($D$) versus wavelength

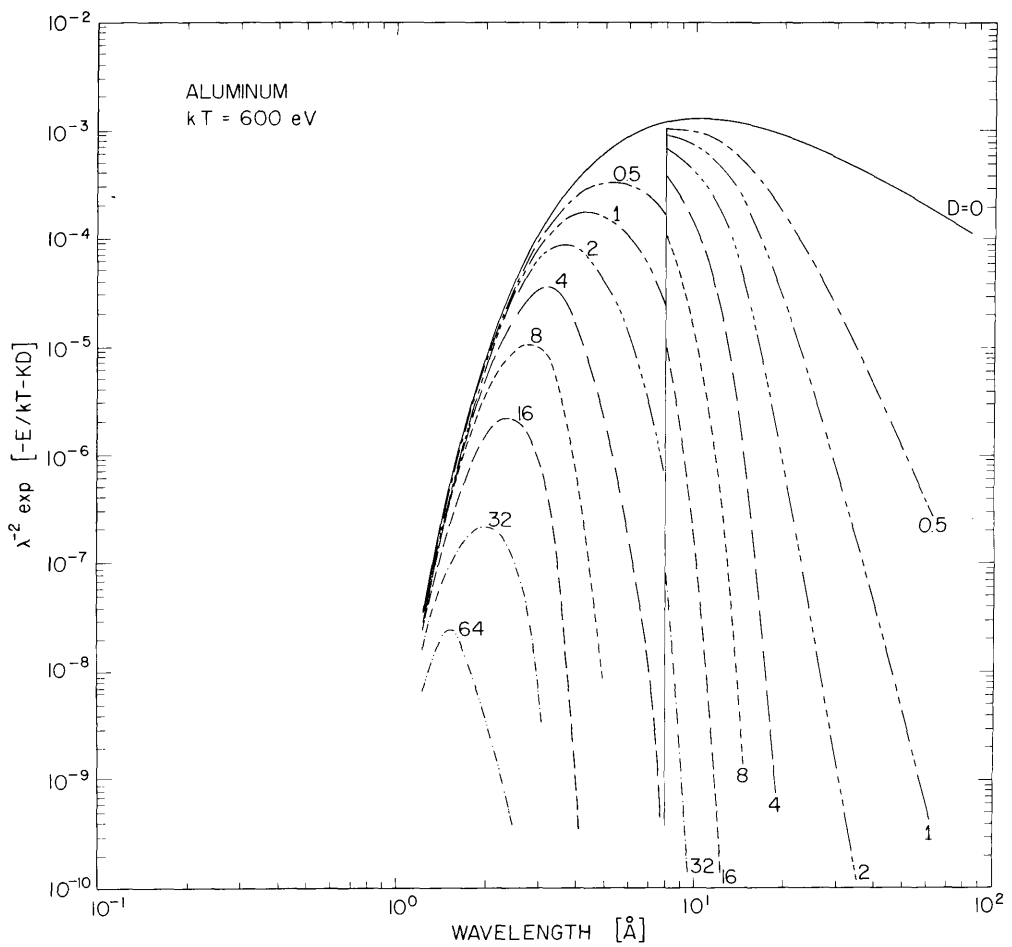


Fig. 7 - Relative bremsstrahlung emission at a temperature ($T$) transmitted through aluminum absorbing foils of thickness ($D$) versus wavelength

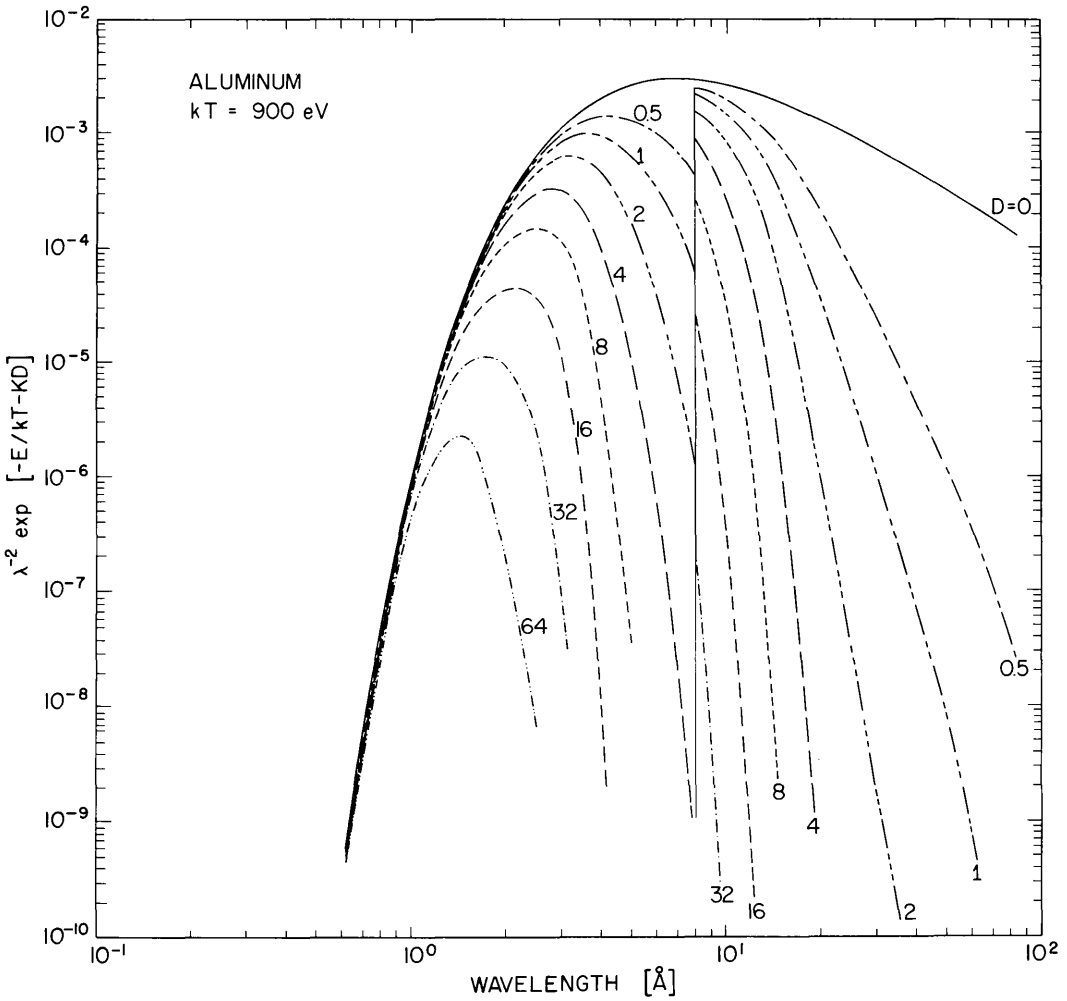


Fig. 8 - Relative bremsstrahlung emission at a temperature ($T$) transmitted through aluminum absorbing foils of thickness ($D$) versus wavelength

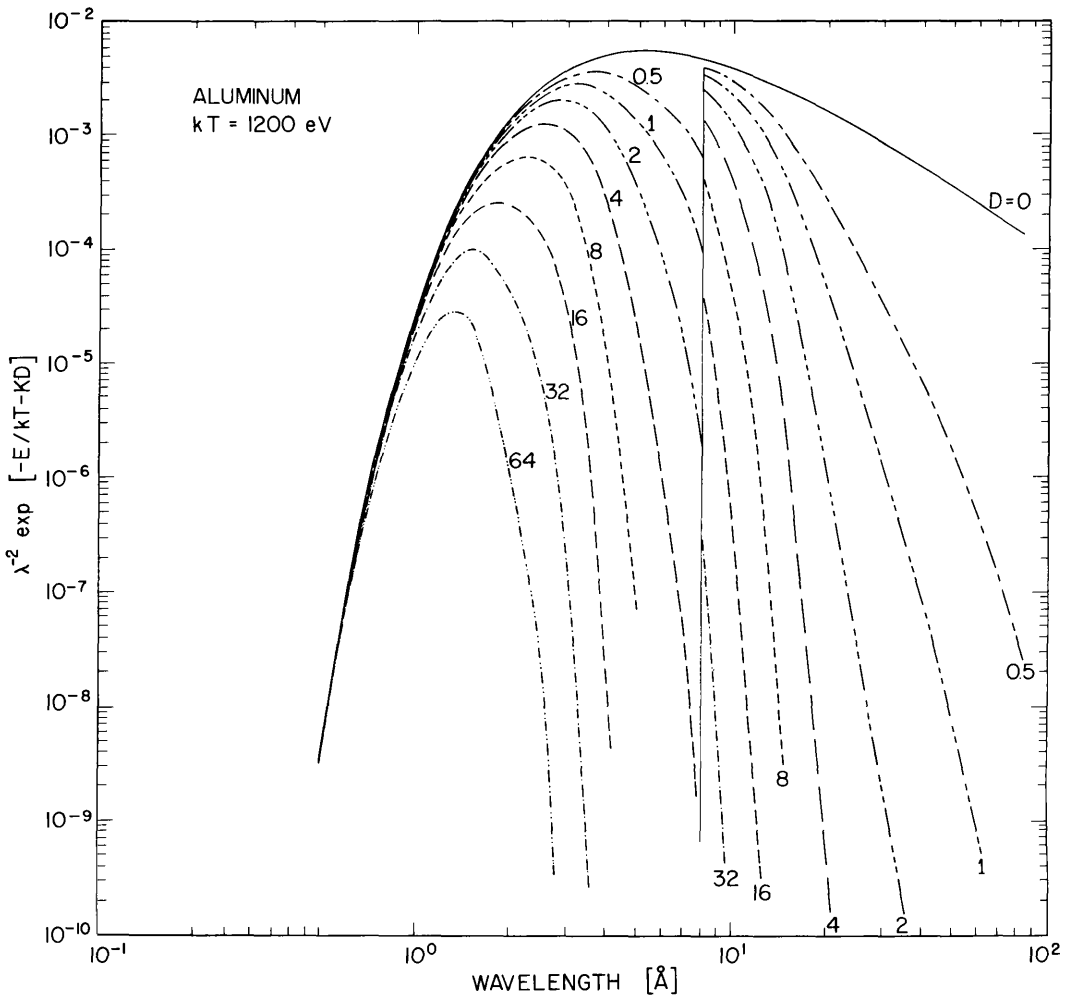


Fig. 9 - Relative bremsstrahlung emission at a temperature ($T$) transmitted through aluminum absorbing foils of thickness ($D$) versus wavelength

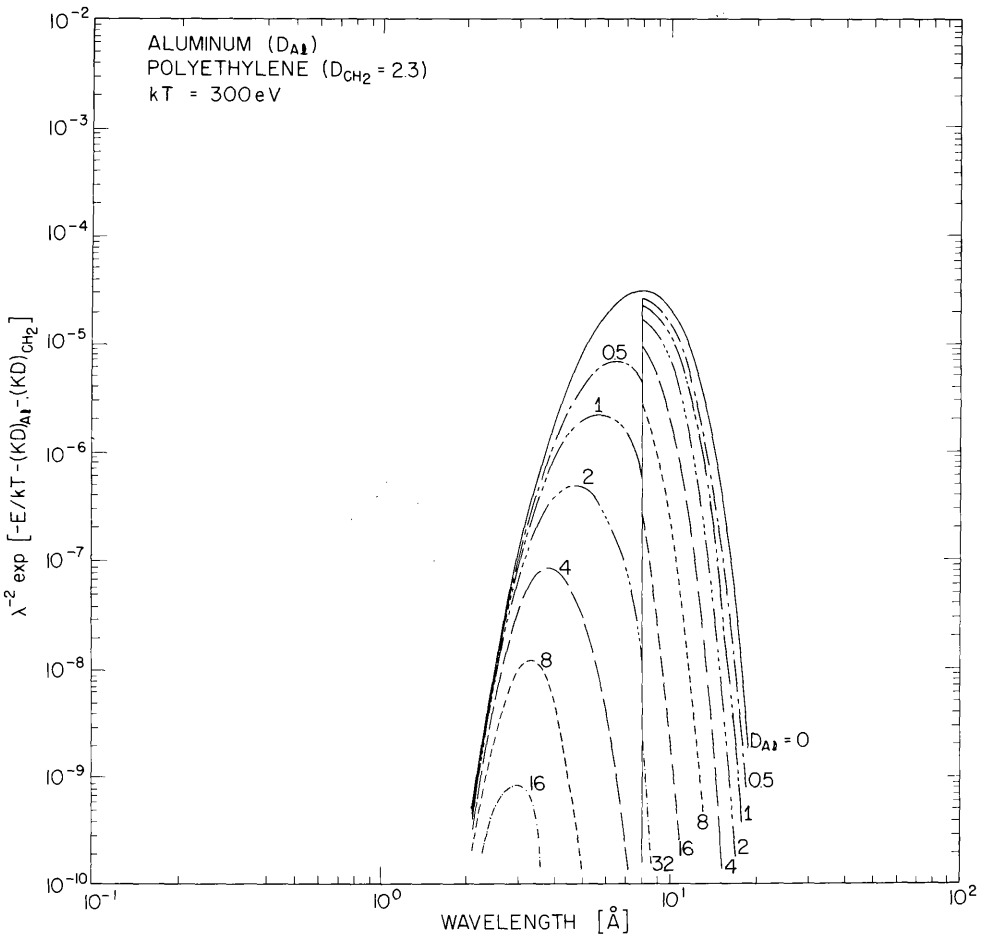


Fig. 10 - Relative bremsstrahlung emission at a temperature ($T$) transmitted through aluminum and polyethylene absorbing foils of thicknesses ($D_{Al}$) and ($D_{CH_2}$) versus wavelength

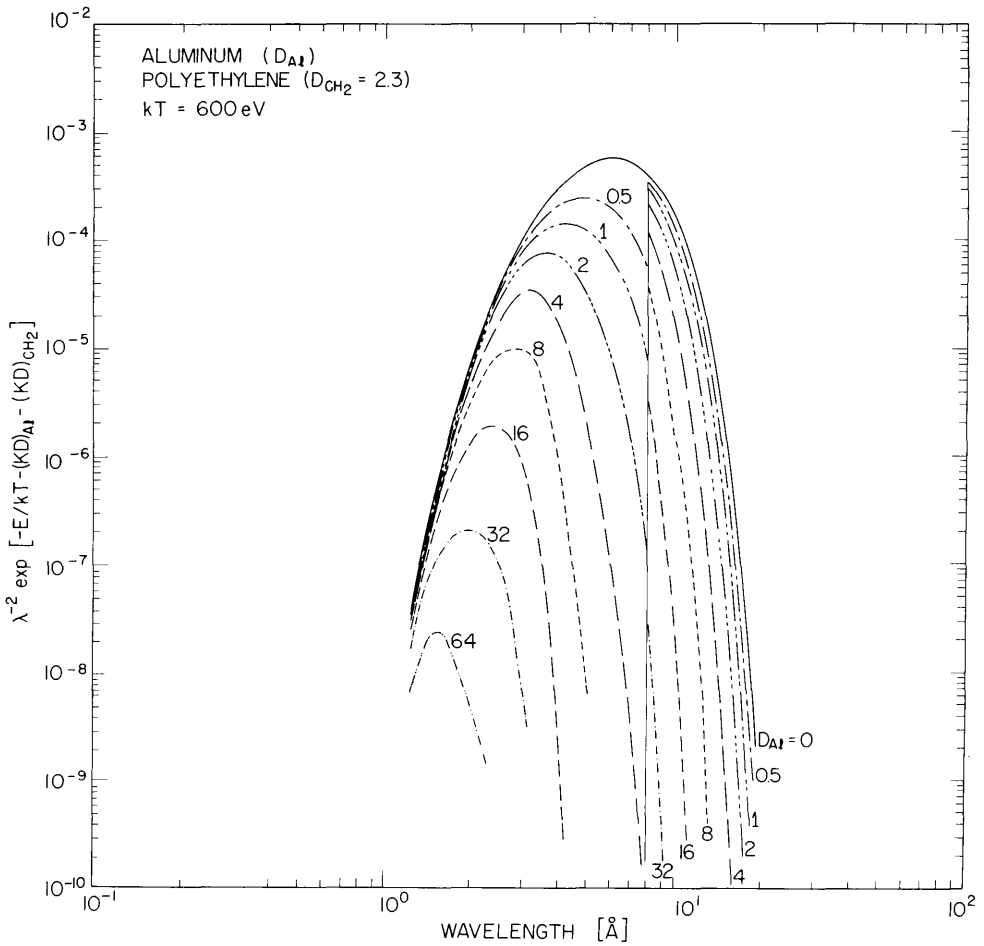


Fig. 11 - Relative bremsstrahlung emission at a temperature ($T$) transmitted through aluminum and polyethylene absorbing foils of thicknesses ($D_{Al}$) and ($D_{CH_2}$) versus wavelength

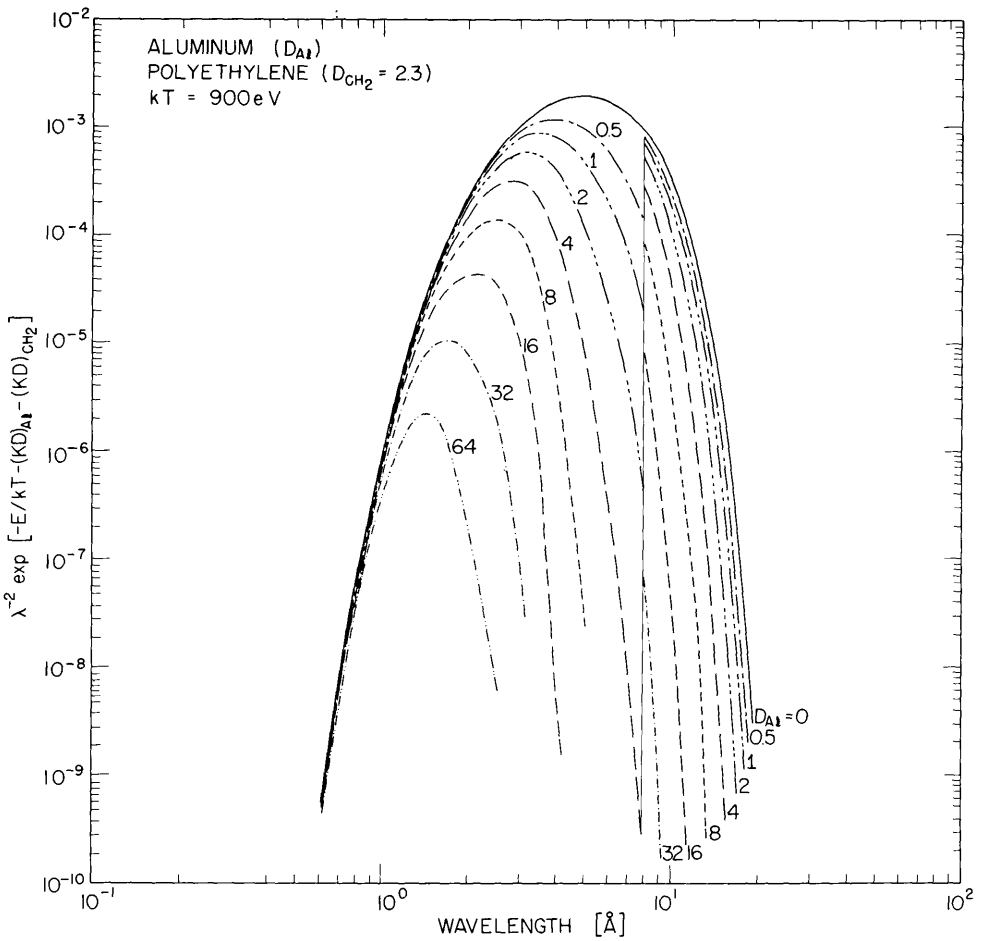


Fig. 12 - Relative bremsstrahlung emission at a temperature ($T$) transmitted through aluminum and polyethylene absorbing foils of thicknesses ($D_{Al}$) and ($D_{CH_2}$) versus wavelength

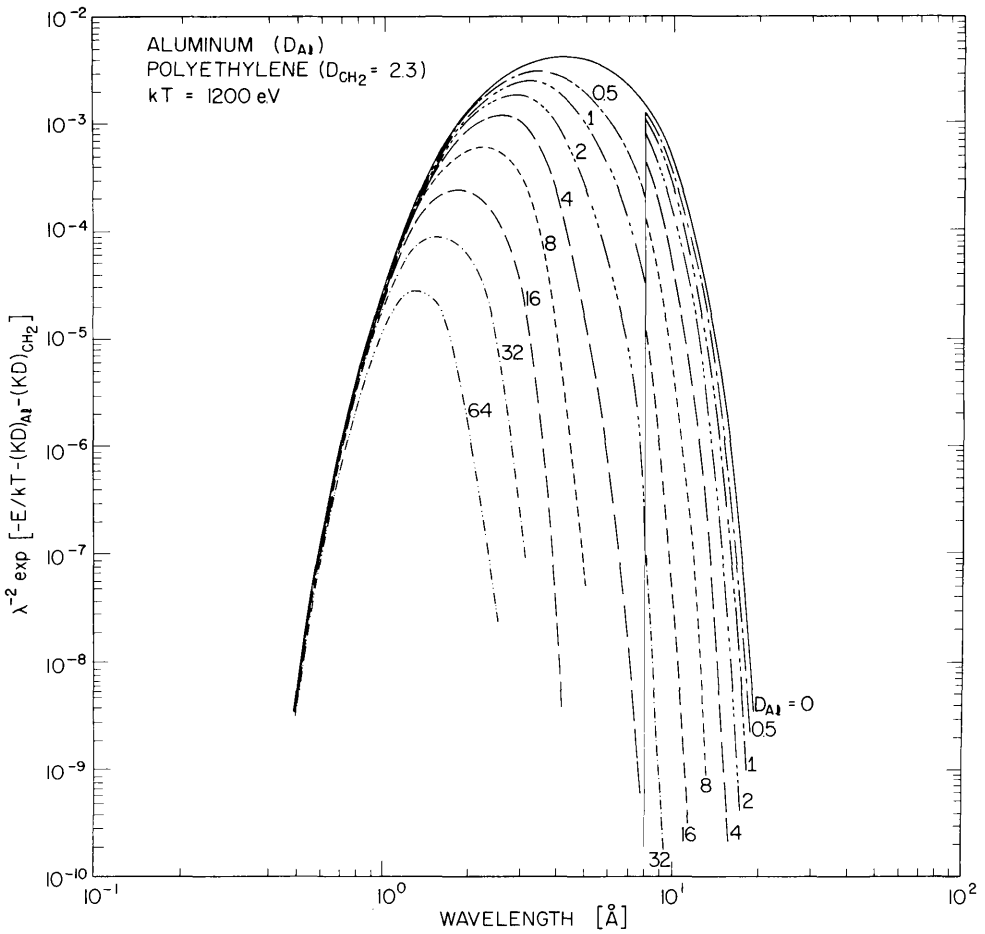


Fig. 13 - Relative bremsstrahlung emission at a temperature ($T$) transmitted through aluminum and polyethylene absorbing foils of thicknesses ($D_{Al}$) and ($D_{CH_2}$) versus wavelength

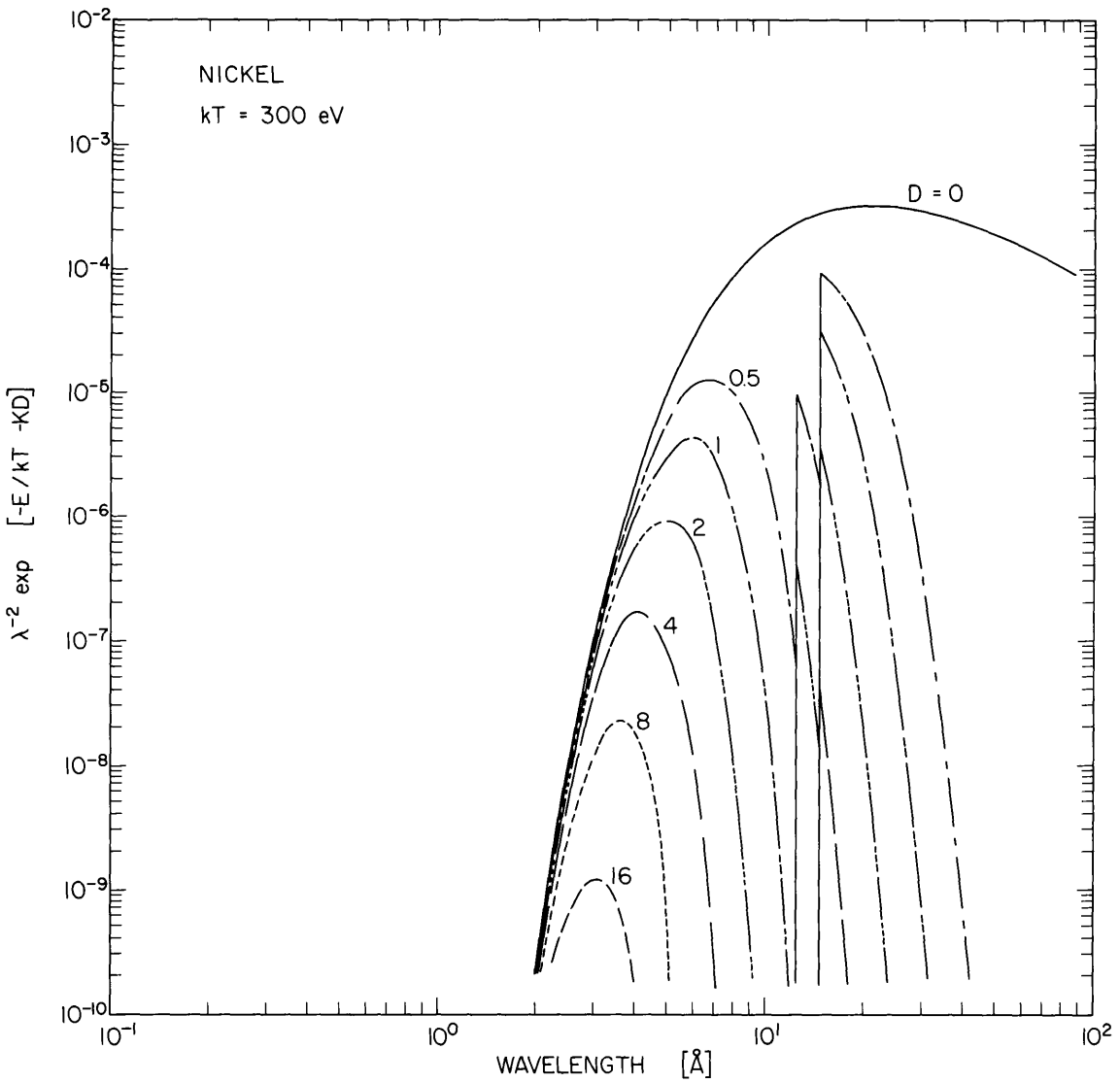


Fig. 14 - Relative bremsstrahlung emission at a temperature ($T$) transmitted through nickel absorbing foils of thickness ($D$) versus wavelength

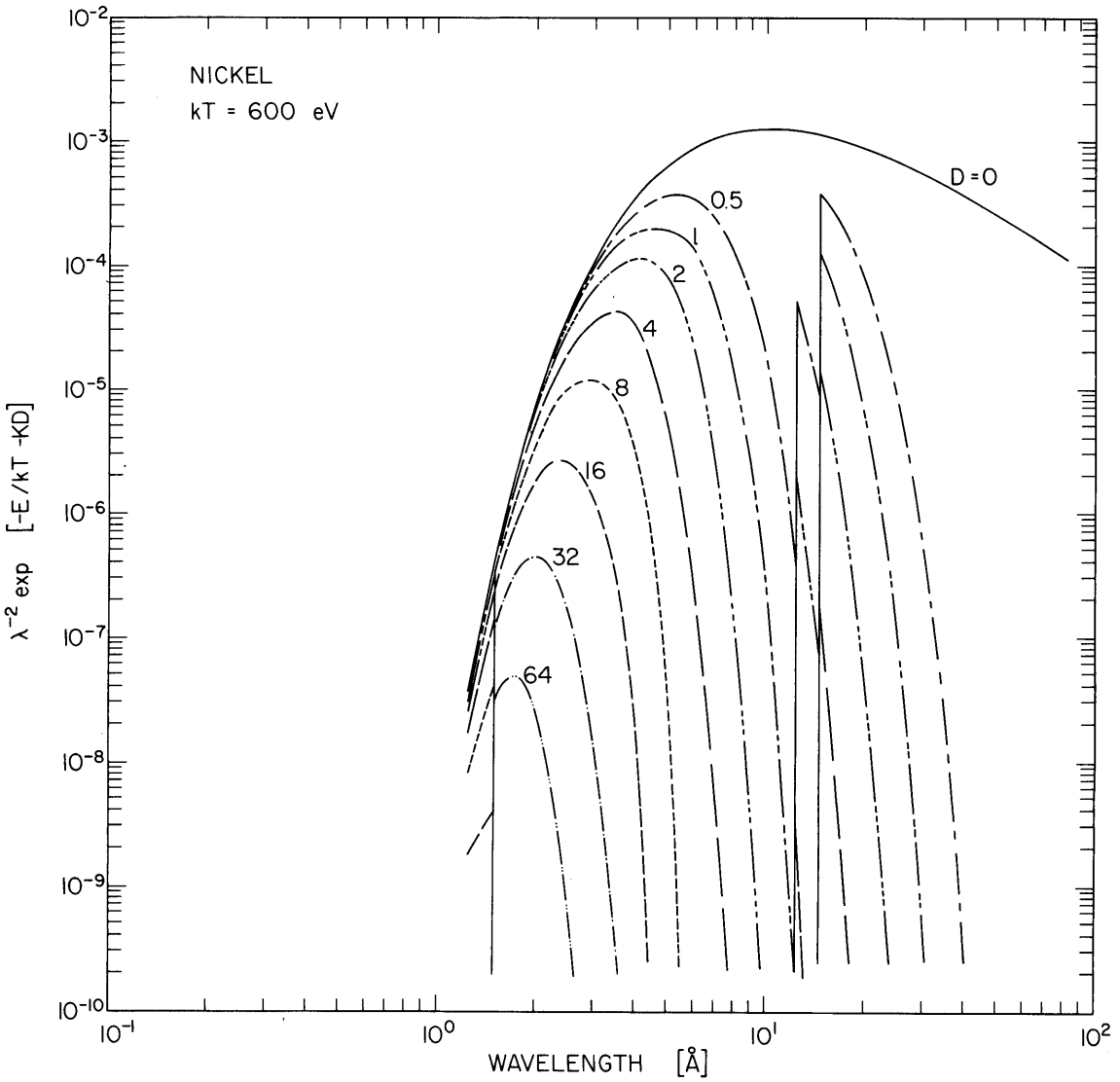


Fig. 15 - Relative bremsstrahlung emission at a temperature ($T$) transmitted through nickel absorbing foils of thickness ($D$) versus wavelength

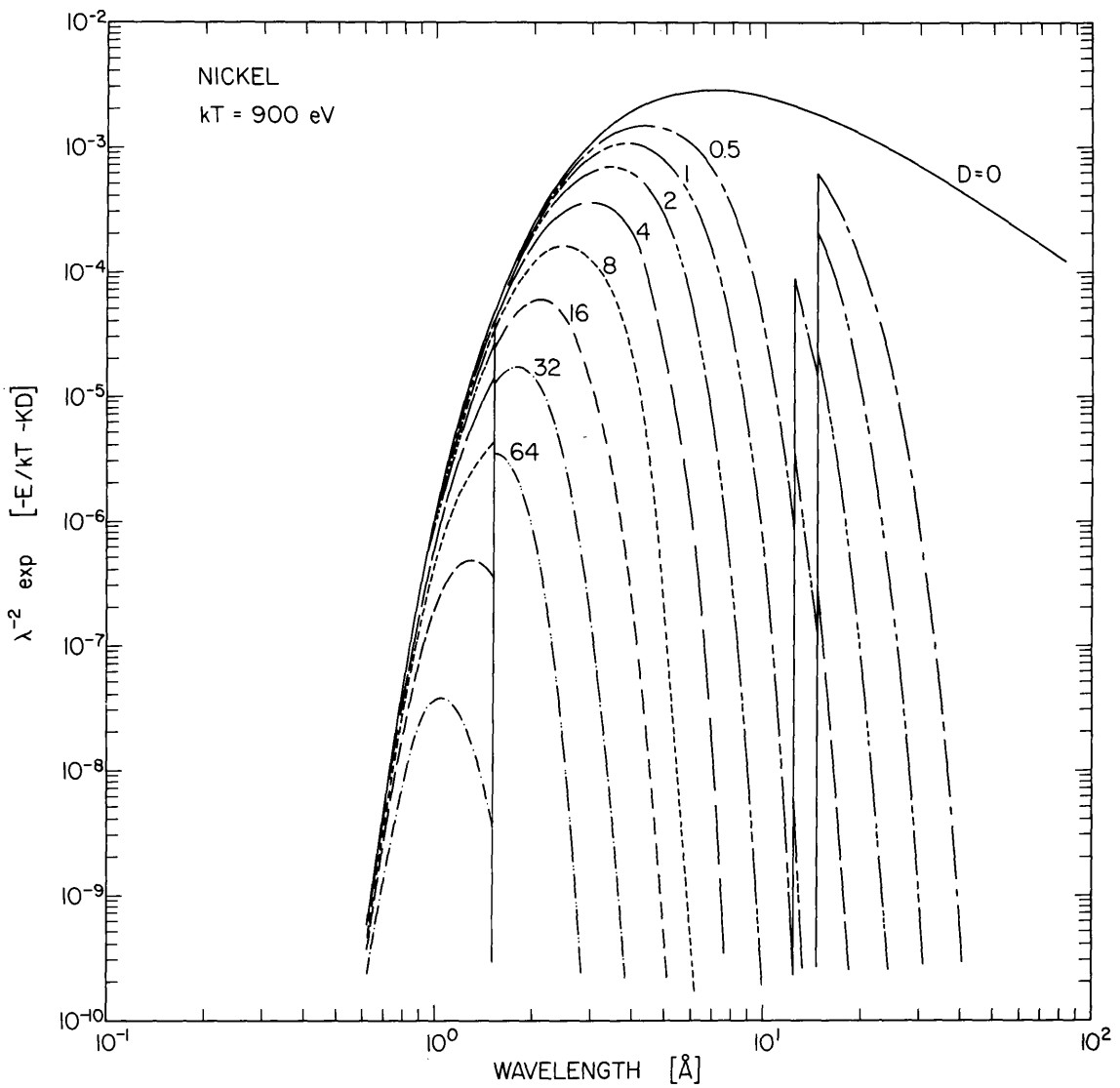


Fig. 16 - Relative bremsstrahlung emission at a temperature ($T$) transmitted through nickel absorbing foils of thickness ($D$) versus wavelength

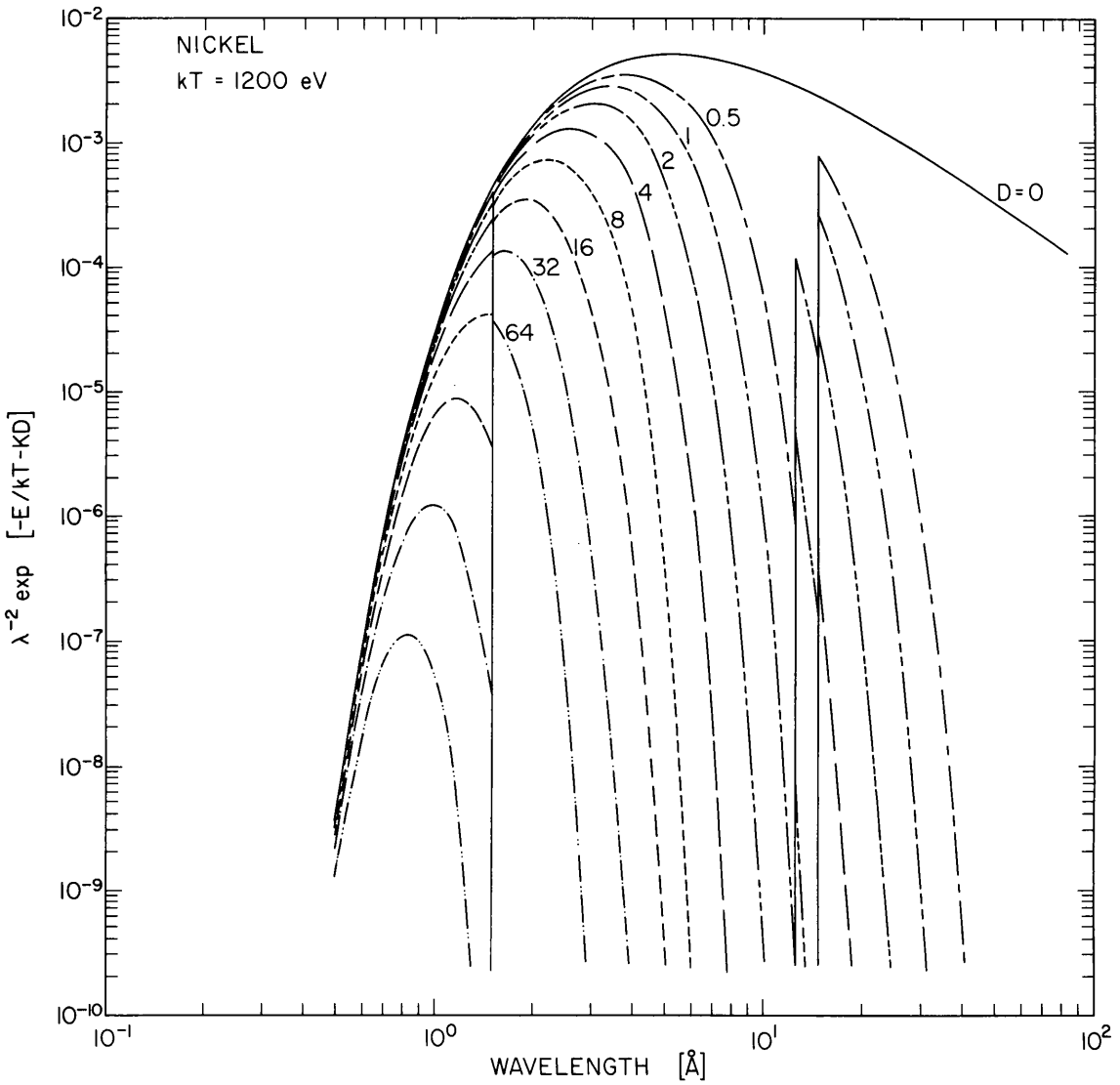


Fig. 17 - Relative bremsstrahlung emission at a temperature ($T$) transmitted through nickel absorbing foils of thickness ($D$) versus wavelength

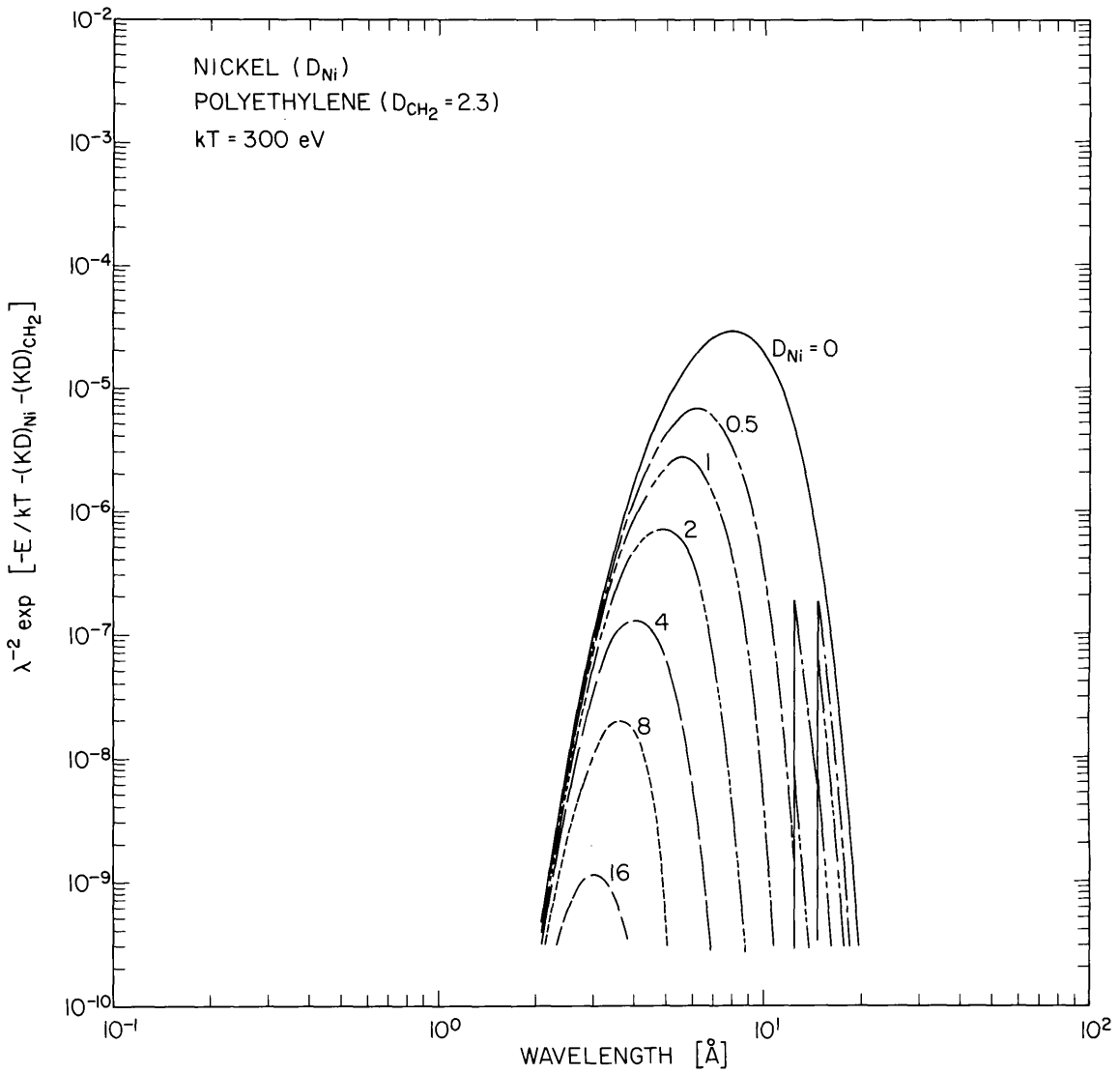


Fig. 18 - Relative bremsstrahlung emission at a temperature ($T$) transmitted through nickel and polyethylene absorbing foils of thickness ($D_{Al}$) and ($D_{CH_2}$) versus wavelength

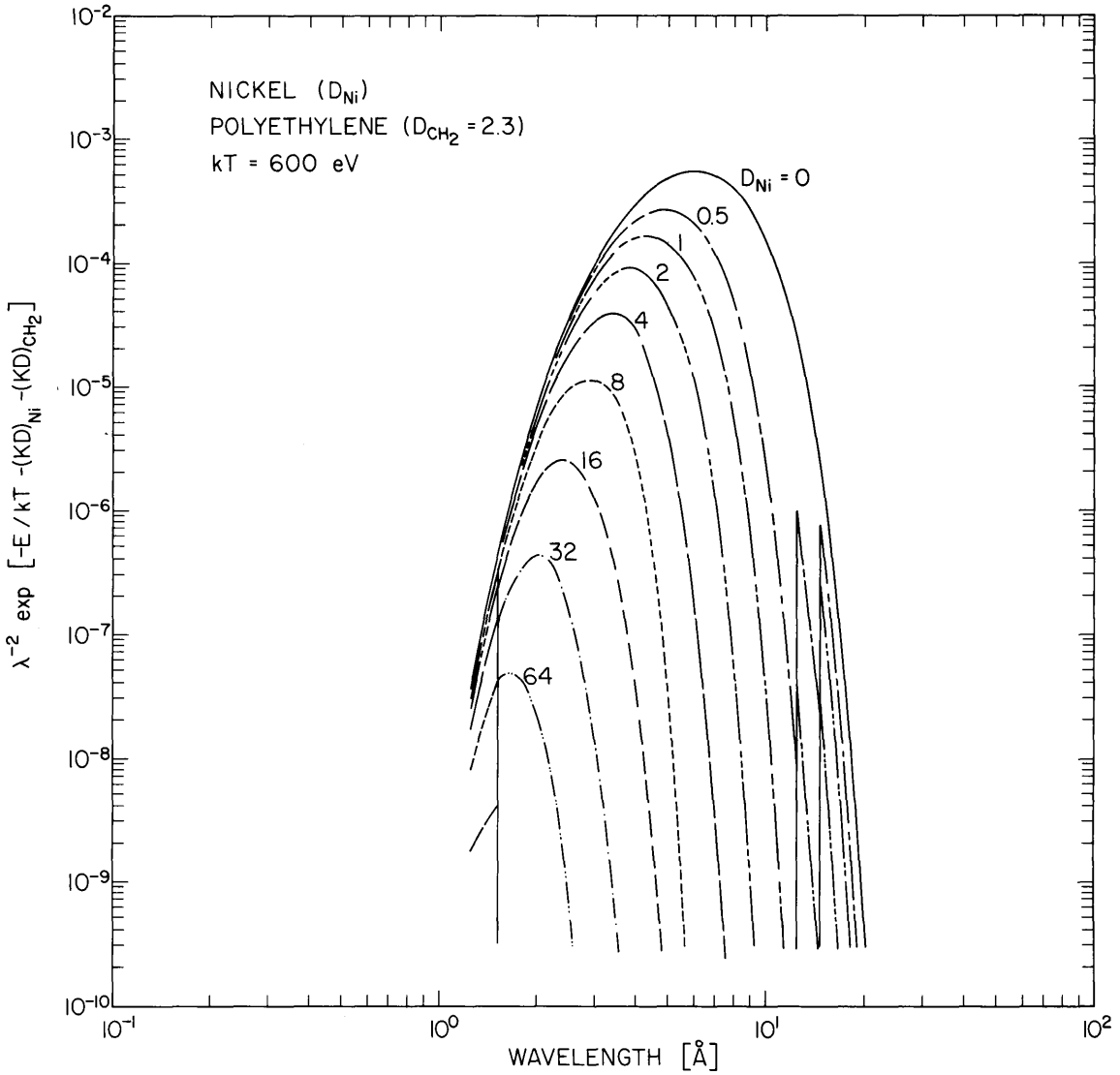


Fig. 19 - Relative bremsstrahlung emission at a temperature ($T$) transmitted through nickel and polyethylene absorbing foils of thickness ($D_{Al}$) and ($D_{CH_2}$) versus wavelength

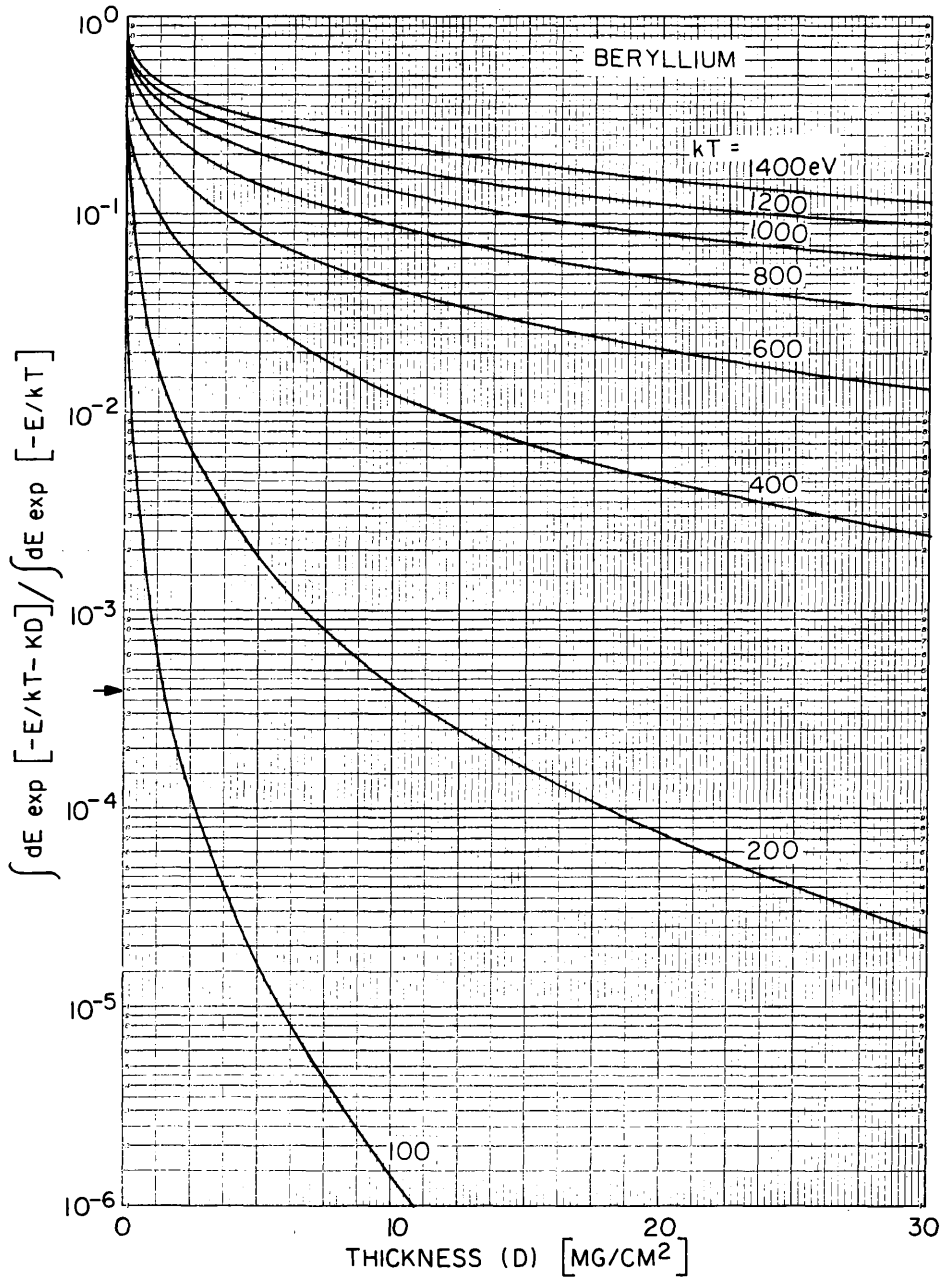


Fig. 22 - Ratio of the integrated bremsstrahlung emission transmitted through beryllium absorbing foils to the total incident flux versus foil thickness (in mg/cm$^2$) for various temperatures. From this data, ordinate values for different thicknesses may be plotted versus temperature and used for plasma electron temperature determination; e.g., see Figs. 28 and 29.

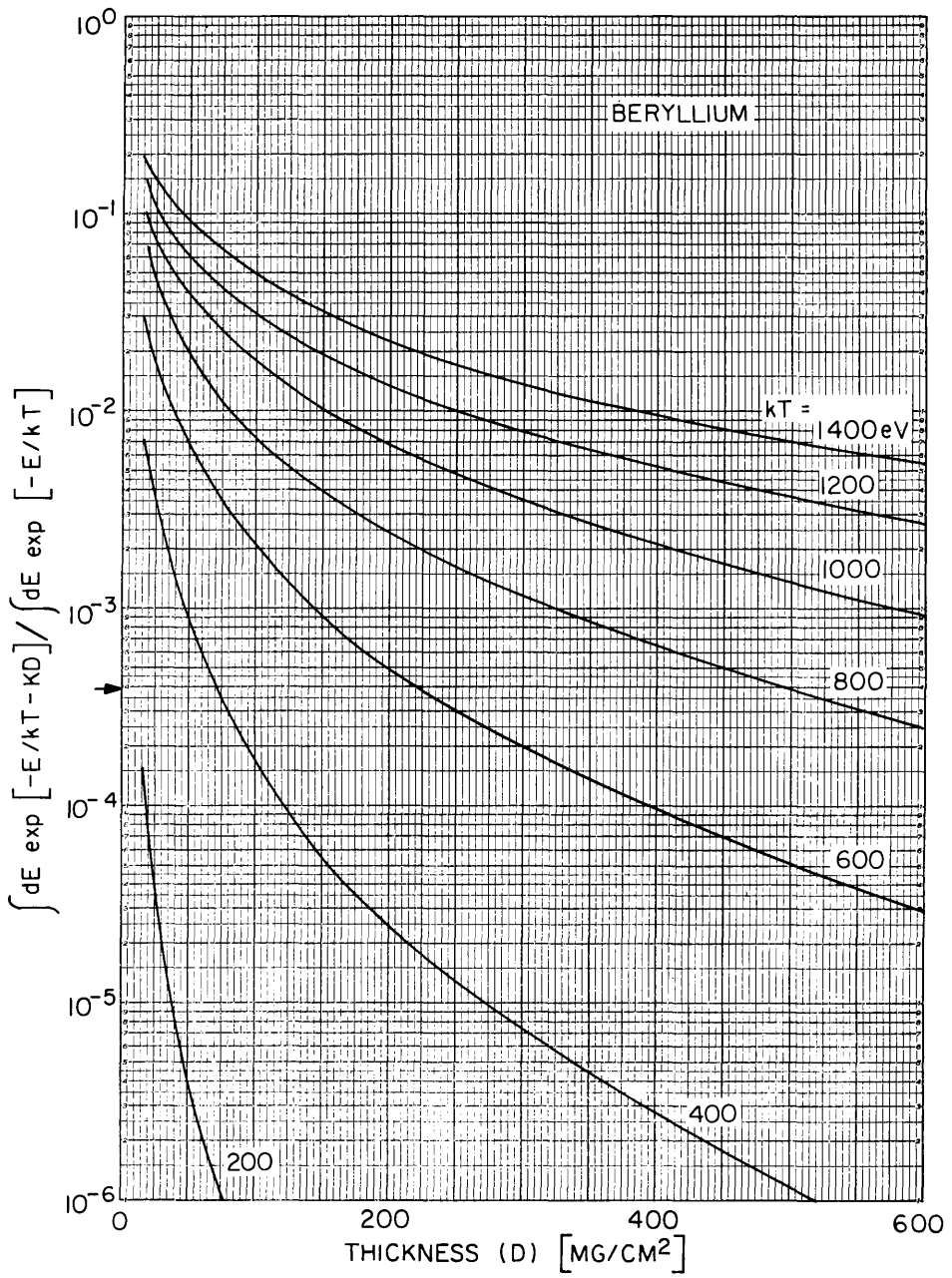


Fig. 23 - Ratio of the integrated bremsstrahlung emission transmitted through beryllium absorbing foils to the total incident flux versus foil thickness (in mg/cm$^2$) for various temperatures. From this data, ordinate values for different thicknesses may be plotted versus temperature and used for plasma electron temperature determination; e.g., see Figs. 28 and 29.

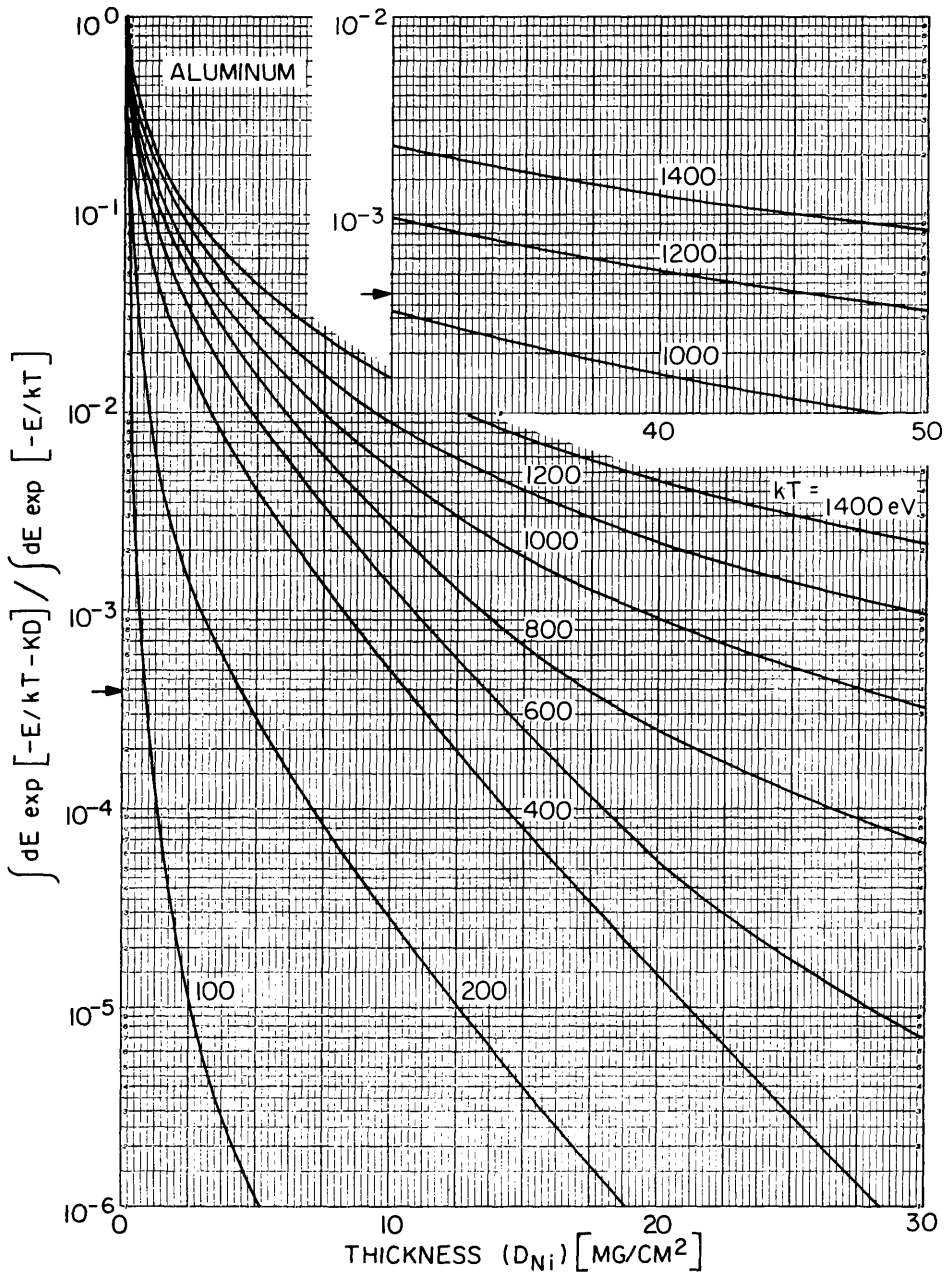


Fig. 24 - Ratio of the integrated bremsstrahlung emission transmitted through aluminum absorbing foils to the total incident flux versus foil thickness (in mg/cm$^2$) for various temperatures. From this data, ordinate values for different thicknesses may be plotted versus temperature and used for plasma electron temperature determination; e.g., see Figs. 28 and 29.

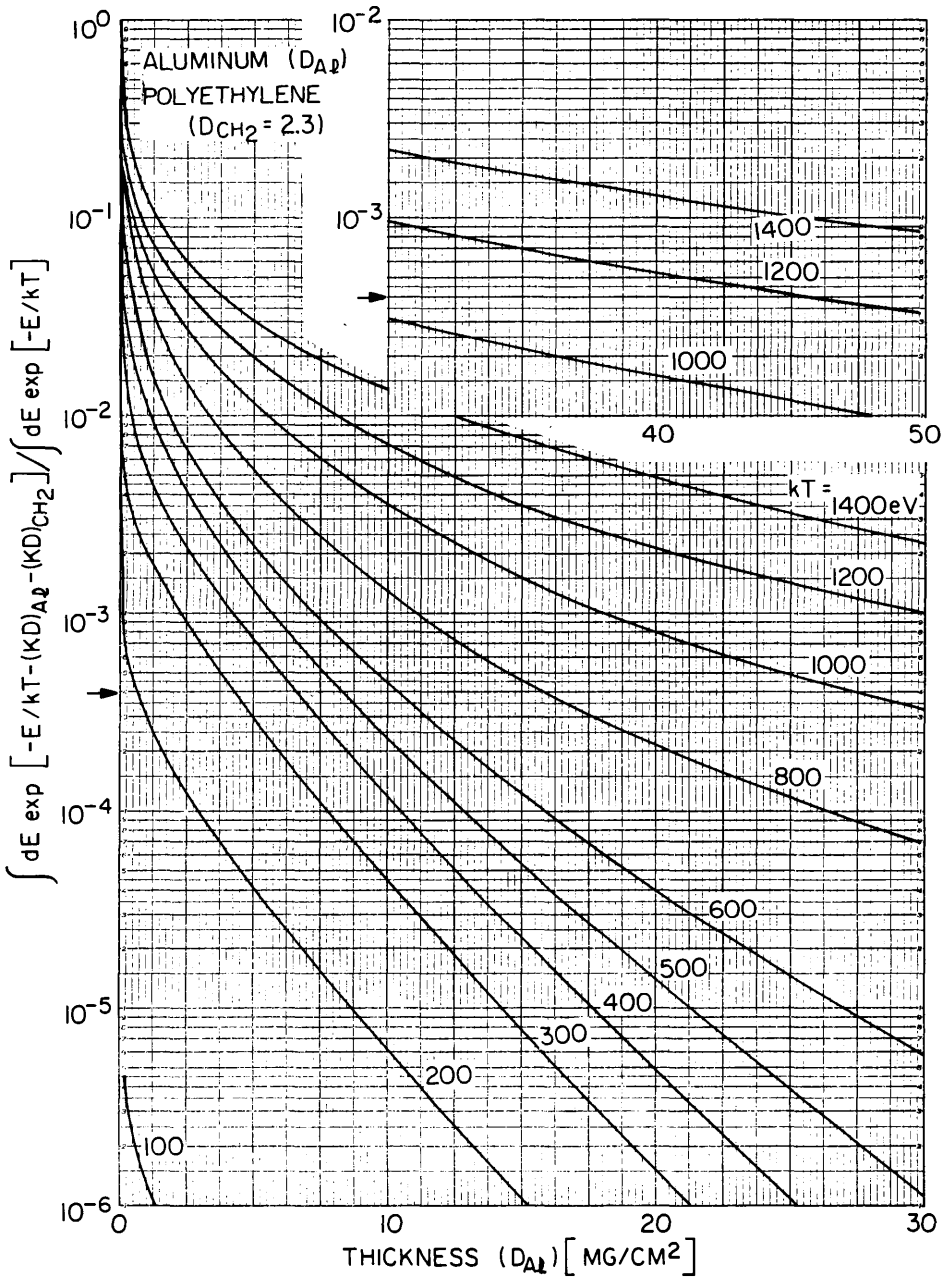


Fig. 25 - Ratio of the integrated bremsstrahlung emission transmitted through aluminum and polyethylene absorbing foils to the total incident flux versus aluminum foil thickness (in mg/cm$^2$) for various temperatures. From this data, ordinate values for different thicknesses may be plotted versus temperature and used for plasma electron temperature determination; e.g., see Figs. 28 and 29.

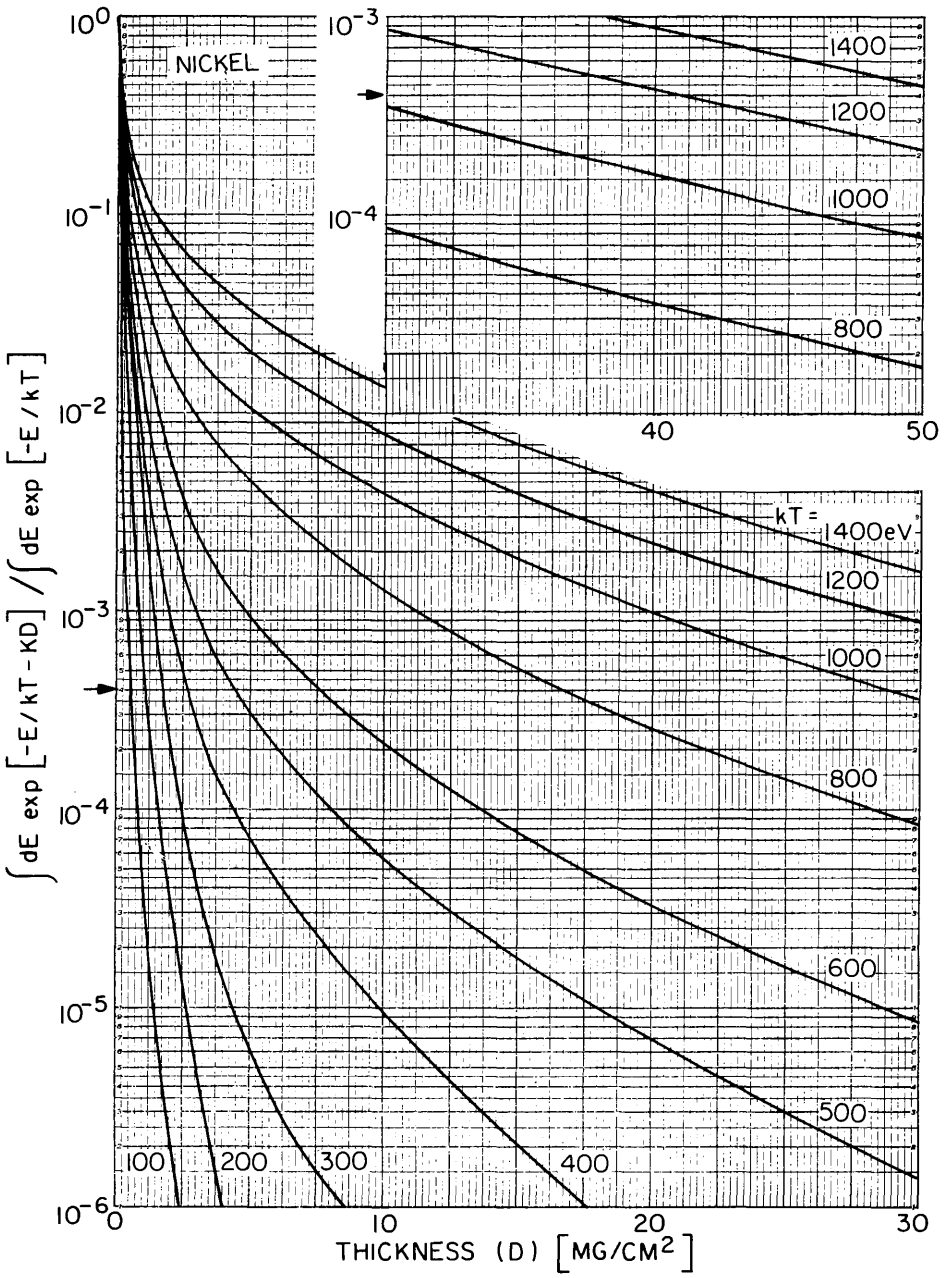


Fig. 26 - Ratio of the integrated bremsstrahlung emission transmitted through nickel absorbing foils to the total incident flux versus foil thickness (in mg/cm$^2$) for various temperatures. From this data, ordinate values for different thicknesses may be plotted versus temperature and used for plasma electron temperature determination; e.g., see Figs. 28 and 29.

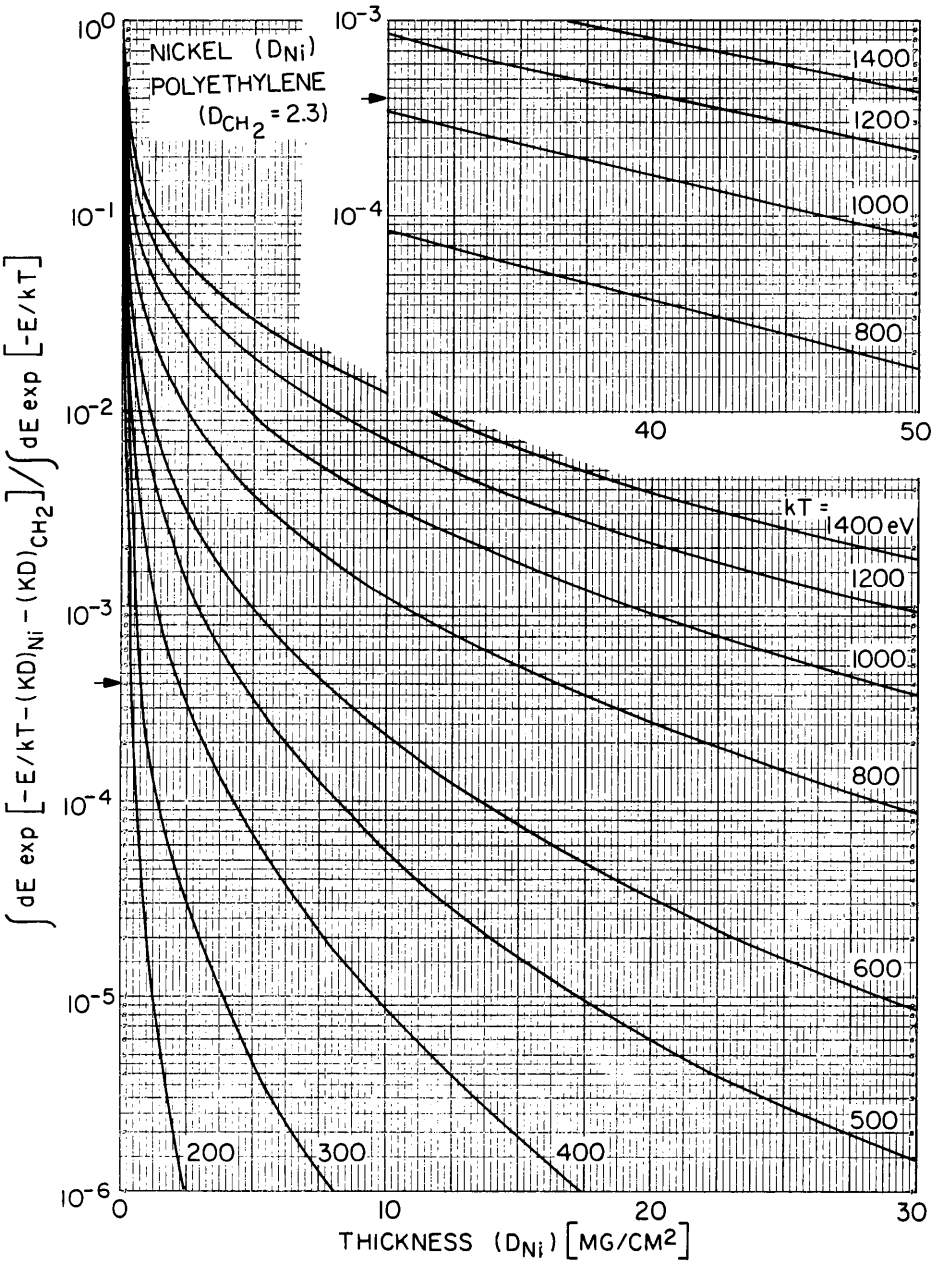


Fig. 27 - Ratio of the integrated bremsstrahlung emission transmitted through nickel and polyethylene absorbing foils to the total incident flux versus nickel foil thickness (in mg/cm$^2$) for various temperatures. From this data, ordinate values for different thicknesses may be plotted versus temperature and used for plasma electron temperature determination; e.g., see Figs. 28 and 29.

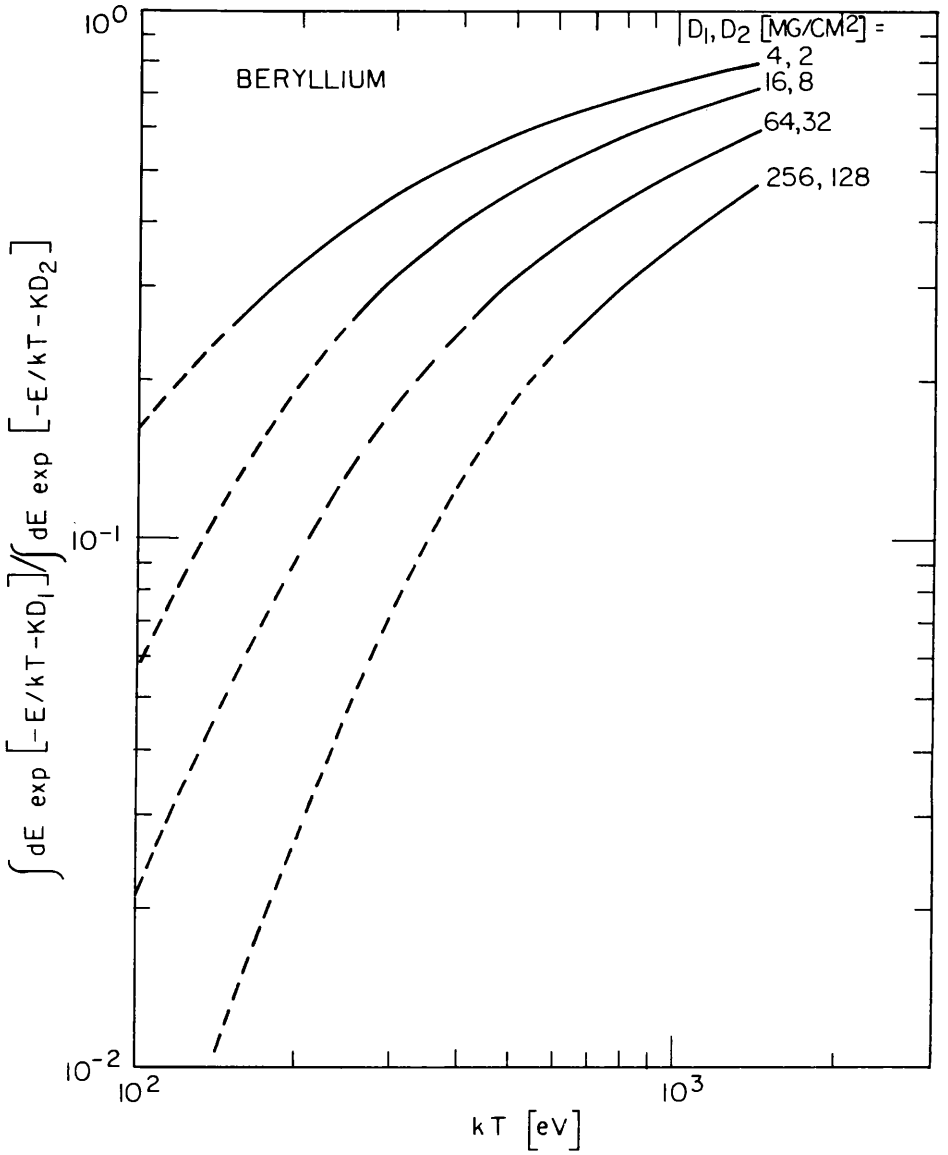


Fig. 28 - Ratio of bremsstrahlung radiation transmitted through beryllium foils of thicknesses $D_1$ and $D_2$ versus temperature, useful in determining plasma electron temperature. This is a typical example of what may be obtained from the results in Figs. 22 through 27.

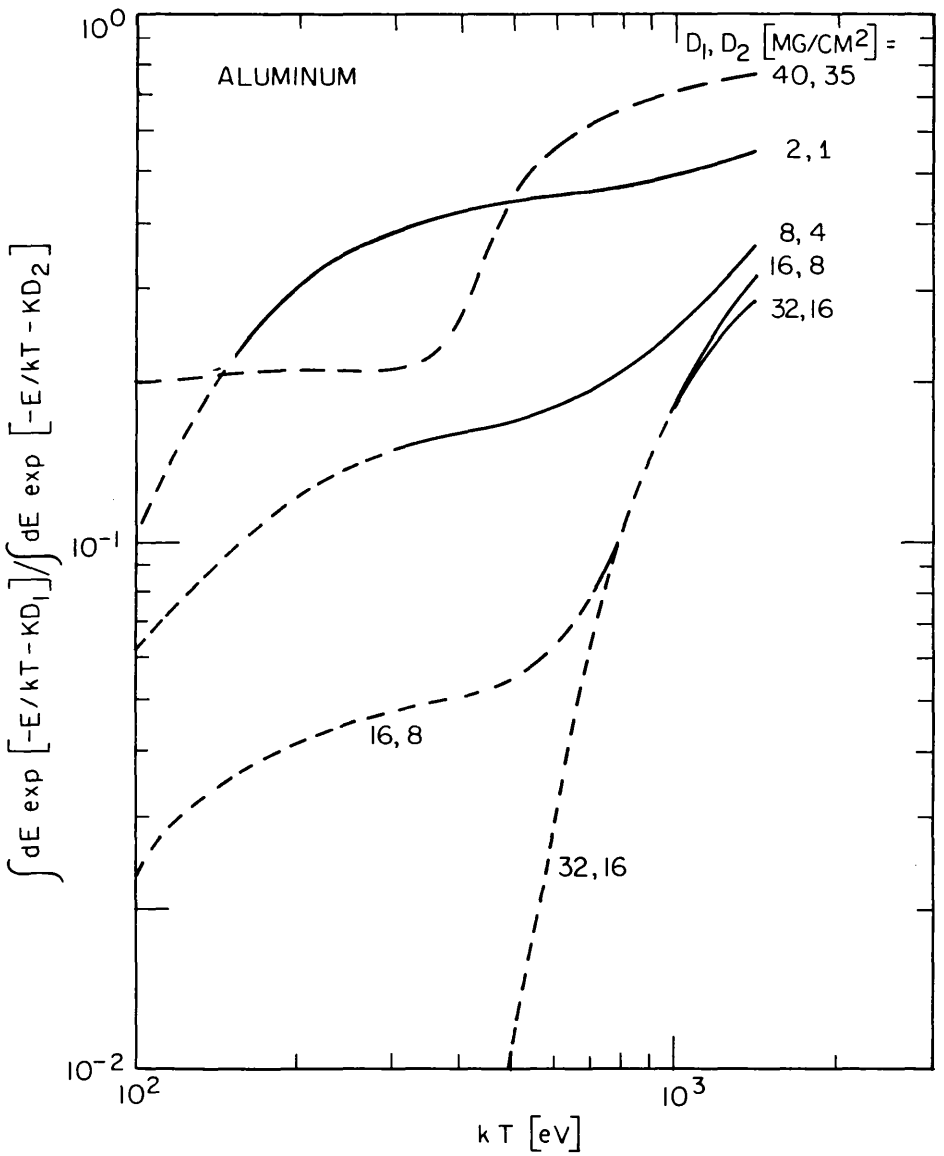


Fig. 29 - Ratio of bremsstrahlung radiation transmitted through aluminum foils of thicknesses $D_1$ and $D_2$ versus temperature, useful in determining plasma electron temperature. This is a typical example of what may be obtained from the results in Figs. 22 through 27.

This page intentionally left blank.

Security Classification

## DOCUMENT CONTROL DATA - R & D

*(Security classification of title, body of abstract and indexing annotation must be entered when the overall report is classified)*

| | |
|---|---|
| 1. ORIGINATING ACTIVITY *(Corporate author)*<br>Naval Research Laboratory<br>Washington, D.C. 20390 | 2a. REPORT SECURITY CLASSIFICATION<br>Unclassified<br>2b. GROUP |

3. REPORT TITLE

CALCULATIONS USEFUL IN THE DETERMINATION OF ELECTRON TEMPERATURE FROM X-RAY CONTINUUM RADIATION EMITTED FROM HIGH TEMPERATURE PLASMAS

4. DESCRIPTIVE NOTES *(Type of report and inclusive dates)*

A final report on one phase of the problem.

5. AUTHOR(S) *(First name, middle initial, last name)*

Raymond C. Elton and Arlo D. Anderson

| | | |
|---|---|---|
| 6. REPORT DATE<br>March 31, 1967 | 7a. TOTAL NO. OF PAGES<br>38 | 7b. NO. OF REFS<br>10 |
| 8a. CONTRACT OR GRANT NO.<br>NRL Problem H02-24<br>b. PROJECT NO.<br>ONR RR 002-10-45-5054<br>c.<br>d. | 9a. ORIGINATOR'S REPORT NUMBER(S)<br>NRL Report 6541<br>9b. OTHER REPORT NO(S) *(Any other numbers that may be assigned this report)* | |

10. DISTRIBUTION STATEMENT

Distribution of this document is unlimited.

| | |
|---|---|
| 11. SUPPLEMENTARY NOTES | 12. SPONSORING MILITARY ACTIVITY<br>Department of the Navy (Office of Naval Research), Washington, D.C. 20360 |

13. ABSTRACT

The results of calculations of the total integrated bremsstrahlung radiation passing through absorbing foils of beryllium, aluminum, and nickel [as well as aluminum and nickel in combination with carbon (polyethylene)] are presented for various temperatures and a range of useful thicknesses. Such information is necessary in obtaining values for the electron temperature in a plasma from measurements of the soft x-ray continuum emission. The spectral distribution of the transmitted radiation is also presented for use in determining the spectral region observed, thereby avoiding regions of undesirable radiation. An indication of an observable flux level in a typical experiment is given, along with equations suitable for scaling to other plasma conditions, as a further aid in selecting foils for a particular application.

DD FORM 1 NOV 65 1473 (PAGE 1)

S/N 0101-807-6801



Security Classification

Security Classification

| 14. KEY WORDS | LINK A ROLE | LINK A WT | LINK B ROLE | LINK B WT | LINK C ROLE | LINK C WT |
|---|---|---|---|---|---|---|
| Plasmas | | | | | | |
| X-Ray Bremsstrahlung | | | | | | |
| Recombination continuum radiation | | | | | | |
| X-Ray Transmission curves | | | | | | |
| Electron temperature | | | | | | |
| Thin metallic foils | | | | | | |

DD FORM 1 NOV 65 1473 (BACK)
(PAGE 2)



Security Classification